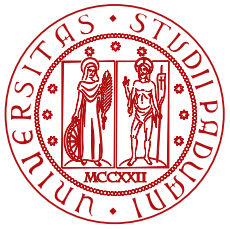

UNIVERSITÀ DEGLI STUDI DI PADOVA

DIPARTIMENTO DI INGEGNERIA DELL'INFORMAZIONE

UNIVERSITÀ DEGLI STUDI DI PADOVA

DEPARTMENT OF INFORMATION ENGINEERING

Master Thesis in Bioengineering

Models of glucagon control on endogenous glucose production

Supervisor

Prof. Chiara Dalla Man

Master Candidate

Alessio Tonello

Academic Year
2022/2023

Graduation Date
06/03/2023

Abstract

The transition from prediabetes to Type 2 Diabetes Mellitus (T2DM) is characterized by defects in insulin secretion and glucagon suppression in response to glucose. However, simultaneous estimation of both hormones actions on endogenous glucose production (EGP) remains a challenge. A mathematical model that fulfill this need, may be helpful to better describe the pathophysiology of T2DM. In particular, it would be useful to understand how and how much impaired glucagon secretion influences the progression of the disease from a prediabetes condition. To address this, we studied 36 non-diabetic subjects on 2 occasions when endogenous hormone secretion was inhibited by somatostatin. Glucagon was infused at 0.65 ng/kg/min, at 0 min to prevent a fall in its concentration (non-suppressed day - NS) or at 120 min to create a transient fall (suppressed day - S). [3-3H]-glucose was infused to mimic an oral glucose challenge together with a prandial insulin infusion – one group received the full dose (1.0 Ins group), another 80% (0.8 Ins group) and another 60% (0.6 Ins group). We tested mathematical models describing EGP as a function of glucose, insulin and glucagon concentrations. Both linear and non linear interactions between hormones were tested. The optimal model assumes that EGP is suppressed by the linear actions of glucose, its rate of change and insulin in a remote compartment, while plasma glucagon stimulated EGP through a parameter that represent hepatic glucagon sensitivity (S_{Gn}). The glucagon evanescent effect was included in the model. With 60% insulin replacement (corresponding to severely impaired insulin secretion), S_{Gn} was significantly higher than with 80% (slightly impaired) and 100% replacement (p-value = 0.024). This demonstrates that glucagon action on EGP is modulated by insulin concentrations, emphasizing the need to quantify secretion and action of both hormones when measuring postprandial pancreatic islets function.

Sommario

La transizione da una condizione di prediabete allo sviluppo del diabete mellito di tipo due (T2DM) è caratterizzata da una compromissione della secrezione di insulina e della soppressione del glucagone in risposta al glucosio. Tuttavia, la stima simultanea dell' azione di entrambi gli ormoni sulla produzione endogena di glucosio (EGP) resta una sfida. Un modello matematico che soddisfa questa richiesta potrebbe aiutare a comprendere meglio la patofisiologia del T2DM. In particolare, considerando come l'imperfetta secrezione di glucagone influenza la progressione della malattia da una condizione di prediabete. Per risolvere questo problema, abbiamo studiato 36 pazienti non diabetici in due occasioni, dove la secrezione endogena di ormoni era inibita dalla somatostatina. Il glucagone è stato infuso a 0.65 ng/kg/min, a 0 min per prevenire un calo della sua concentrazione (giorno non soppresso - NS) o a 120 min per creare una riduzione momentanea (giorno soppresso - S). [3-3H]-glucosio è stato infuso mimando un carico orale di glucosio assieme ad una infusione prandiale di insulina – un gruppo ha ricevuto l'intera dose (gruppo 1.0 Ins), un altro l'80% (gruppo 0.8 Ins) e un altro il 60% (gruppo 0.6 Ins).
Abbiamo testato vari modelli matematici che descrivono l' EGP in funzione delle concentrazioni di glucosio, insulina e glucagone. Sono state testate sia interazioni lineari sia non lineari tra gli ormoni. Il modello ottimale assume che l' EGP sia soppresso da azioni lineari proporzionali al glucosio, la sua derivata e insulina in un compartimento remoto, mentre il glucagone nel plasma stimola l' EGP attraverso un parametro che rappresenta la sensitività epatica al glucagone (S_{Gn}). L'effetto evanescenza del glucagone è stato incluso nel modello. Nel gruppo "0.6 Ins" (che corrisponde a una severa compromissione della secrezione di insulina), S_{Gn} è significativamente più alto che nel gruppo "0.8 Ins" (compromissione leggera) e nel gruppo "1.0 Ins" (p-value = 0.024). Questo dimostra che l'azione del glucagone su EGP è modulata dalla concentrazione di insulina, enfatizzando la necessità di quantificare la secrezione e l'azione di entrambi gli ormoni quando si misura la funzionalità delle isole pancreatiche nel periodo post-pandriale.

Contents

List of Acronyms

AIC Akaike Information Criterion

ANOVA Analysis Of Variance

BIC Bayes Information Criterion

CV Coefficient of Variation

DM Diabetes Mellitus

EGP Endogenous Glucose Production

FDA U.S. Food and Drug Administration

FI Fisher Information

FIM Fisher Information Matrix

FWER Family-Wise Error Rate

GEN-IC Generalized Information Criterion

GIR Glucose Infusion Rate

IFG Impaired Fasting Glucose

IGT Impaired Glucose Tolerance

IGS Impaired Glucagon Suppression

MLE Maximum Likelihood Estimator

NGT Normal Glucose Tolerance

NS Not Suppressed

S Suppressed

SA Specific Activity

STD Standard Deviation

OGTT Oral Glucose Tolerance Test

PDF Probability Distribution Function

T1DM Type 1 Diabetes Mellitus

T2DM Type 2 Diabetes Mellitus

TTR Tracer to Tracee Ratio

WNLLS Weighted Non Linear Least Squares

WRSS Weighted Residual Sum of Squares

1 Introduction

1.1 The glucose-insulin-glucagon system

Glucose is a monosaccharide, a simple sugar that is the primary source of energy of the body. It is metabolized by all tissues to fuel their activities. Based on their glucose uptake, they can be classified in two groups. *Glucose dependent tissues*, such as the brain and the red blood cells, need a continuous and fix sugar intake, that is around $150\ g$ per day in a normal subject [1]. *Insulin dependent tissues*, like adipose and muscular tissues, in which glucose utilization depends on insulin, since the transport of glucose inside the cell is performed by a glucose transporter called GLUT-4, which is synthesized only if insulin is present. **Insulin** is a hormone (a chemical messenger) secreted by the β-cells of the islets of Langerhans, which are regions of the pancreas. Insulin is released into the hepatic portal vein and after a liver extraction, it reaches the circulation. The pancreas is able to sense plasma glucose concentration and to adjust insulin secretion to it. Besides controlling glucose uptake, insulin influences the endogenous glucose production (EGP) that mainly comes from the liver. In particular, insulin inhibits EGP. Also the liver is a glucose-sensing organ. Consequently, it can adjust EGP according to the glucose level in the blood. Another hormone that has a role in the system is **glucagon**, that is secreted by the α-cells of the islets of Langerhans. Like insulin, glucagon is released into the hepatic portal vein and cleared by the kidneys [2]. Its main physiological action is to stimulate the hepatic glucose production. Also glucagon secretion is regulated by plasma glucose concentration.

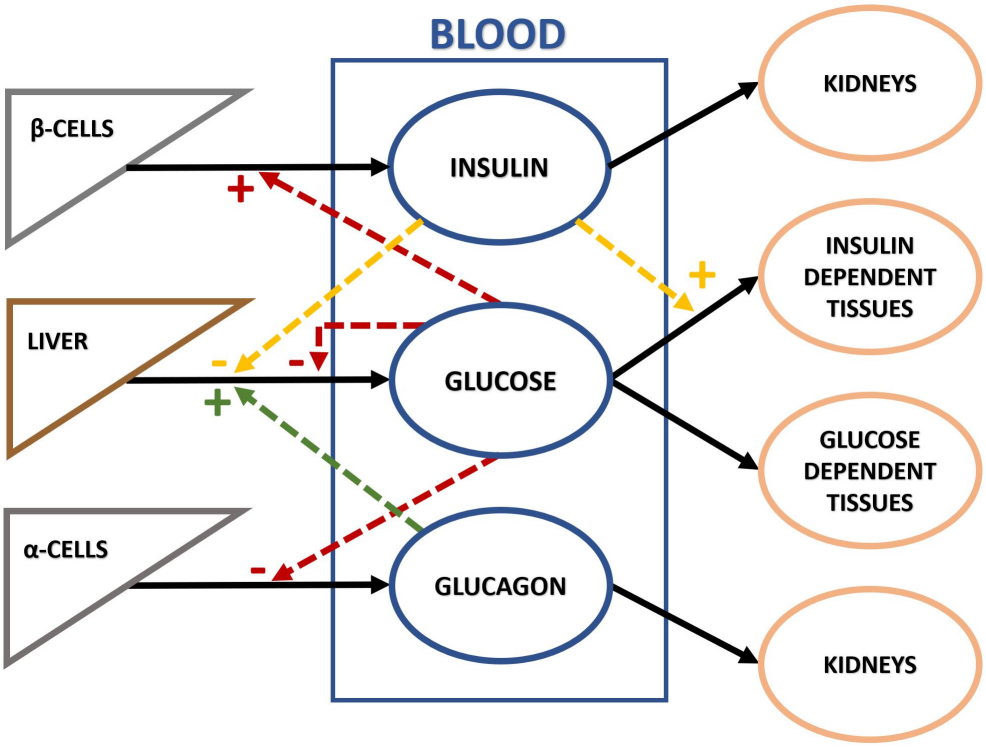

Figure 1.1: Schematic representation of the glucose regulatory system. Glucose is endogenously produced by the liver and released into circulation. A glucose rise inhibits its own production, stimulates β-cells to produce insulin and reduces the glucagon secretion from α-cells. Both hormones are released into the circulation. The metabolic action of insulin is to reduce EGP and to increase the uptake of glucose from insulin dependent tissues. Conversely, glucagon stimulates the liver to secrete more glucose. Thus, **insulin and glucagon are antagonist hormones.**

The aim of this complex system is to maintain *glycaemia*, the blood glucose level, inside a safety range, the *euglycemia* condition. As seen before, the glucose dependent tissues require a constant intake of glucose. Consequently, if blood glucose is not enough to fulfill the need, such tissues does not work properly. This condition is called *hypoglycemia* and it can lead to really dangerous conditions in the short term, like coma or even death. Hypoglycemia arises when blood glucose is below 70 $[mg/dl]$. The opposite condition is, in turn, another risky scenario. When glycaemia is too high (glucose above 180 $[mg/dl]$, called *hyperglycemia* condition) several bad complications, e.g. cardiovascular diseases, hypertension and retinopathy, may occur in the long term. As briefly described above, the body realizes the homeostasis of blood glucose level by means of a complex feedback mechanism, that is the result of interactions among glucose, insulin and glucagon on their target tissues (figure 1.1).

Endogenous glucose production (EGP)

This thesis will focus on hormones action on EGP. Thus, a more detailed explanation of the related physiology is presented.
The liver produces glucose through two processes: *glycogenolysis* and *gluconeogenesis*. Glycogenolysis is the degradation of *glycogen*, a polysaccharide of glucose that is stored inside the liver, into glucose-1-phosphate; via dephosphorylation by the enzyme glycogen phosphorylase. Than, glucose-1-phosphate is converted to glucose-6-phosphate by the enzyme phosphoglucomutase [3]. A final reaction, promoted by the enzyme glucose 6-phosphatase, converts glucose-6-phosphate into glucose.
The second primary mechanism used by the body to maintain blood sugar level is gluconeogenesis. The generation of glucose is the result of a metabolic pathway that uses non-carbohydrate carbon substances, like glycerol, lactate, glutamine and alanine to realize glucose-6-phosphate. Gluconeogenesis occurs also in the kidneys, however the liver is the major contributor of EGP from both processes [4]. As highlighted before, insulin inhibits glucose production; nevertheless, its action only affect glycogenolysis [5]. The primary effect of glucagon on the liver is promoting glycogenolysis, enhancing the enzyme glycogen phosphorylase [6]. Gluconeogenesis is stimulated by glucagon only during prolonged hypoglycemia (more than 3 hours) [7]. Moreover, glucagon inhibits the synthesis of glycogen from blood glucose (glycogenesis). A continuous glucagon stimulation of the liver produces an effect that wanes over time. This physiological phenomenon is called *glucagon evanescent effect* [8]. The causes of the reduction of glucagon action are still not clear. A possible reason is the desensitization of receptors regulated by cyclic adenosine monophosphate (cAMP), that are responsible of the hepatic signaling cascade triggered by glucagon [9]. Another reason might be the depletion of hepatic glycogen or a stimulus mediation of the hypothalamus [10]. Otherwise, it may be a combination of all these phenomena. A representation of the glucagon action on the liver is illustrated in figure 1.2.
There is also a relation between glucagon and insulin actions. In fact, glucagon stimulation on EGP dependents on insulin level. When plasma insulin concentration is high, the hepatic response to glucagon is mitigated [11]. Conversely, it seems that ambient glucose level does not influence glucagon action on the liver [12].

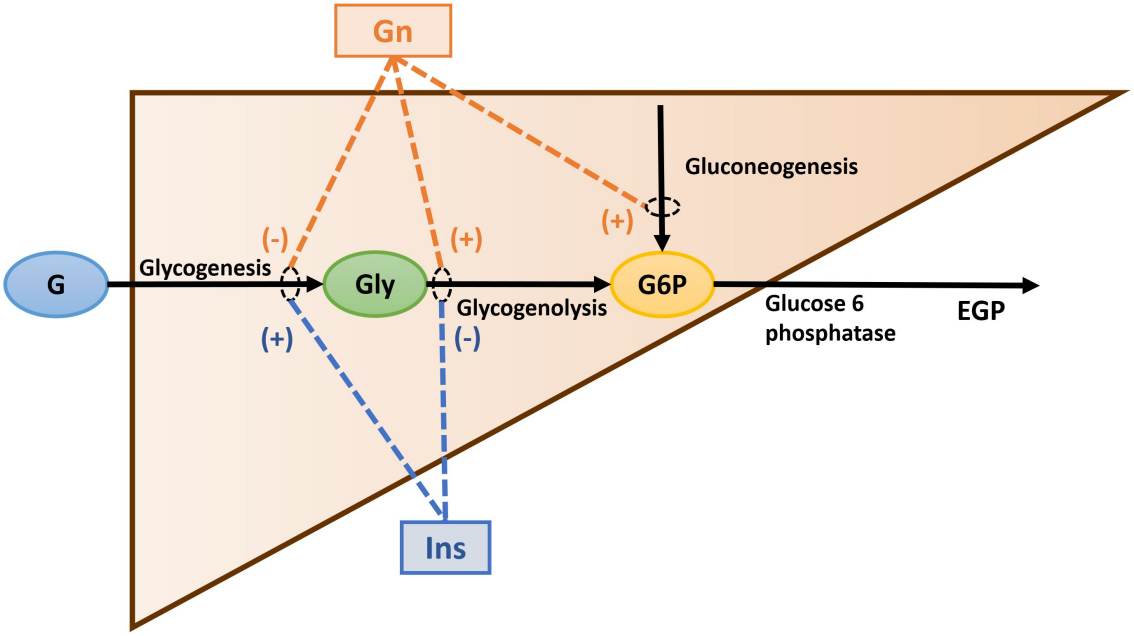

Figure 1.2: Simplified version of glucagon (Gn) and insulin (Ins) action model on the liver. Glucagon stimulates endogenous glucose (G) production (EGP) increasing glycogenolysis and gluconeogenesis and inhibiting glycogenesis. Insulin action reduces EGP via glycogenolysis inhibition, and promotes filling of glycogen (Gly) reserves enhancing glycogenesis. Glucose-6-phosphate (G6P) is converted into glucose and secreted into circulation thanks to enzyme glucose 6-phosphatase.

Diabetes mellitus

As seen before, the aim of the glucose regulatory system is to maintain glucose homeostasis and so, to avoid hypoglycemia and hyperglycemia conditions. When the human body is not able to properly control blood sugar level, it is affected by a chronic disorder, called *Diabetes mellitus (DM)* or simply diabetes. There are two types of diabetes. *Type 1 diabetes mellitus (T1DM)* is caused by an autoimmune destruction of the β-cells of the pancreas. Consequently, there is absence of endogenous insulin secretion. It affects around 5%-10% of all patients with DM and it is typically diagnosed in children and adolescents [13]. *Type 2 diabetes mellitus (T2DM)* is distinguished by impaired glucagon suppression (IGS) and defective insulin secretion in the postprandial period (after the consumption of a meal). It is caused by a mix of genetic variations and environmental factors. Obesity, ageing, unhealthy and sedentary lifestyle are risk factors for the development of T2DM [14]. In the U.S. alone, T2DM is expected to increase by more than 50% in 2030 with respect to 2015. DM is considered a global pandemic and a major health crisis with the need of

increasing medical and societal costs [15]. A metabolic state in between an healthy condition and T2DM is called *prediabetes*. It is characterized by increased plasma glucose concentrations both during fasting and after a two hours standard 75 g oral glucose tolerance test (OGTT). In particular, Impaired Fasting Glucose (IFG) subjects have fasting blood sugar level between 5.6 and 6.9 [mmol/l] and Impaired Glucose Tolerance (IGT) subjects have a blood glucose between 7.8 and 11.0 [mmol/l] after 2h from OGTT. To prevent DM development, it is essential to understand which factors are predominant risks of conversion from prediabetes to T2DM. Consequently, understanding the pathophysiology of the glucose regulatory system is crucial. In non-diabetic subjects, a lack of postprandial glucagon suppression combined with a reduced and delayed secretion of insulin caused hyperglycemia [16]. The same happens in patients with type 2 diabetes after an oral test [17]. As a result, also in pathological conditions, glucagon and insulin actions interact. In fact, abnormal glucagon suppression has an effect on EGP only in presence of severely impaired insulin secretion. Moreover, α-cell dysfunction is also associated with genetic variant in the TCF7L2 gene [18]. Thus, it becomes clear that defective glucagon secretion and its action on the liver is a key factor to monitor in T2DM prevention.

1.2 Quantification of the glucoregulatory system

Quantitative measurements of the glucoregulatory system can be derived with easy calculations but rather complex and invasive experiments. For example, with an approach called *glucose clamp technique* [19], it is possible to calculate a measure of how good insulin is to reduce blood glucose level, the so called *insulin sensitivity (S_i)*. However, to better quantify the mechanisms of glucose regulation in the body, in the past decades it became clear that a model based approach is needed. A model is a mathematical description of the system under analysis that enables the identification of non measurable entities, such as the production of an hormone [20]. This more complex approach gives the possibility to derive more information with simpler experiments (like the OGTT). Exploiting models, it was possible to quantify S_i ([21], [22]), producing an estimation validated against the clamp technique (gold standard) [23]. This formulation assumes that S_i is the combination of two distinct components: the disposal insulin sensitivity S_i^D, i.e. the ability of insulin to promote glucose utilization and the hepatic insulin sensitivity S_i^L, that quantify insulin suppression action on EGP. Several models, that try to estimate separately the two components are present in literature ([24],[25]). However, none of them takes into

account glucagon action on EGP. As seen before, glucagon plays an important role in the system, especially in presence of defective insulin secretion. Not considering its action produces a systematic error in the estimation of S_i^L. In recent years, models that consider both hormone actions on the liver were developed ([12],[26],[27],[28]). Several model structures were used to define the interaction between glucagon and insulin on EGP, with different level of detail (from an overall approach to the description of hormone actions on single processes like glycogenolysis and gluconeogenesis). The experimental design on which these models were based varied substantially and so did also their domain of validity. Moreover, they showcased some limitation in fitting performance or they were not validated. For all this reasons, simultaneous estimation of both hormones actions on EGP remains a challenge.

1.3 Aim of the thesis

The goal of this work is to develop a mathematical model of endogenous glucose production (EGP) to quantify simultaneously hepatic insulin sensitivity S_i^L and hepatic glucagon sensitivity S_{Gn} in presence of different levels of impaired insulin secretion and defective glucagon suppression in the postprandial period. A model pursuing this objective can improve the estimation of insulin action on the liver and better describe the pathophysiology of type 2 diabetes, especially, considering how much impaired glucagon secretion influences the progression of the disease.

1.4 Thesis content

In chapter 2 the experimental design of the study from which data were collected is presented, along with a description on the pre-processing steps used to estimate EGP. Chapter 3 presents linear and non linear mathematical models of EGP tested in this thesis. A brief summary of the whole model identification and assessment procedure is reported in chapter 4. Results and discussion are outlined in chapters 5 and 6, respectively.

2

Material and Methods

2.1 Experimental design

Data used in this thesis come from a study performed by the Division of Endocrinology, Diabetes and Metabolism of Mayo Clinic College of Medicine.
Subjects of the study were chosen if they didn't have history of diabetes and they lived at maximum 100-mile from Mayo Clinic in Rochester, MN. The selection was random and based on their genotype at *TCF7L2* (rs7903146). A match taking into consideration body weight, sex, age and fasting glucose concentration was performed between subjects homozygous for allele TT (diabetes-associated allele) and allele CC (disease-protective allele). Participants undertook an oral glucose tolerance test (OGTT) to identify their glucose tolerance status [29]. Subjects were not taking medications and didn't have history of chronic illness or surgery that could affect the study outcome. From three days before the study, all subjects followed a specific diet (15% protein, 30% fat, 55% carbohydrate).
36 non-diabetic subjects took part in the experiment. They were studied in two different days in which somatostatin inhibited endogenous hormone secretions. Glucose, insulin and glucagon were infused exogenously to control all the inputs relevant to the glucose regulatory system. In particular, subjects received a glucose infusion to mimic the appearance in the circulation of an oral ingestion of 75g of glucose [30]. This glucose infusion was labelled with $[3-^3H]$ glucose, which allows the estimation of endogenous glucose production (EGP) in a virtually model-independent way (section 2.2). Glucagon was infused at a rate of 0.65 [ng/kg/min], at t = 0 [min] to block a drop in glucagon (not suppressed day) or at 120 [min] to produce a temporary fall

in glucagon (suppressed day). In the not suppressed day (NS) the infusion resemble what append in type 2 diabetes patients, with glucagon staying almost constant if not rising. In the suppressed day (S) the infusion mimics what append in an healthy subject after a meal, with glucagon initially falling and then rising.
Participants were divided into three groups, each group received a different insulin infusion. The group "1.0 Ins" received an insulin profile that mimic the secretory response in healthy subject (normal glucose tolerance - NGT). Another group ("0.8 Ins") had an insulin infusion with 80% of the dose of the previous group. The last group ("0.6 Ins") received 60% of the dose of the first group. This partitioning was done to simulated the response of impaired glucose tolerant (IGT) and type 2 diabetic subjects to a glucose challenge. Ideally, the only difference between the non suppressed study (NS) and the suppressed study (S) was the glucagon infusion. All the previous infusions started at a reference time of t = 0 [min]. However, since the goal was to estimate EGP an additional infusion of $[3 - ^3 H]$ glucose was performed from t = -180 [min] respect to the reference time. At t = 0 [min] this infusion was decreased to mimic the anticipated fall in EGP [31]. In figure 2.1 a diagram of the experimental design is shown. More precised details about the performed experiment can be found in the original work [32].

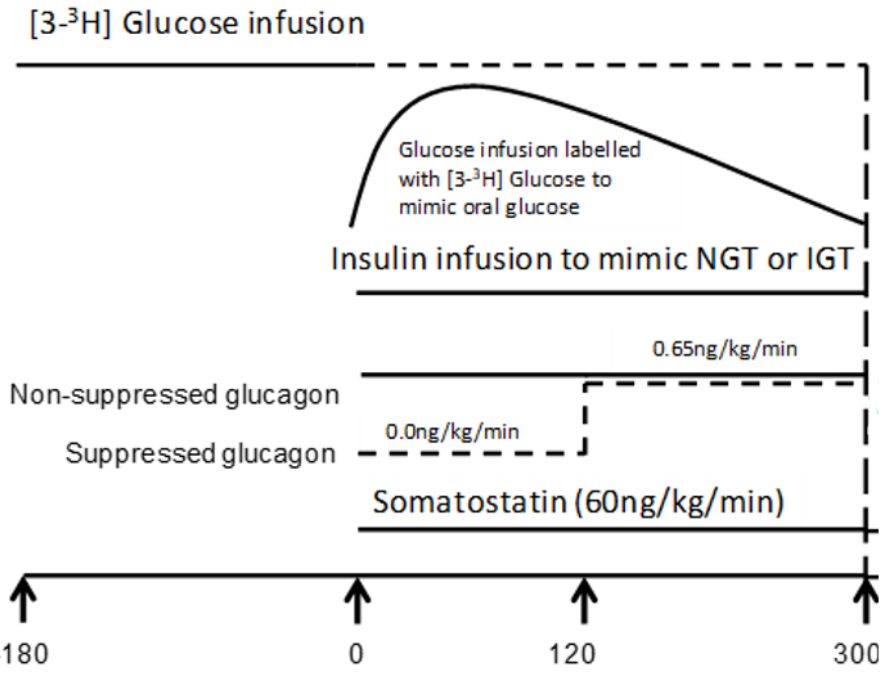

Figure 2.1: Diagram of the administered infusions in both experiments. Dashed line in the continuous glucose tracer infusion indicates a decrease in the infused tracer.

2.2 Model-independent estimate of EGP

The tracer methodology

"A tracer is a substance introduced into a biological organism or other system so that its subsequent distribution may be readily followed from its color, radioactivity, or other distinctive property." [33]. In biology and medicine tracers are used to solve the fundamental problem of describing in a quantitative manner the kinetics of substances present in the body. The use of tracers can help to better understand the production/secretion, the utilization/degradation and the transportation and transformation fluxes of a given compound of interest. Usually, this substance is produced and utilized by the body, it is present is several organs and tissues and there is not the possibility (due to the invasiveness of the experiment, for example) to directly measure the flux of interest. What is generally possible is to measure the concentration of this compound in just one accessible pool, generally the plasma.
An ideal tracer should have the following properties:

- to be detectable by taking a measurement from the system under study;
- the introduction of the tracer into the system must not perturb the system dynamics;
- the body cannot distinguish the tracer from the compound of interest, called tracee.

The last property lead to the following definition, called **tracer-tracee indistinguishably principle**: "the probability that a particle leaving the system is a tracer particle equals the probability that a particle of the system is a tracer particle". Let us make an example to clarify what it means. In this thesis, we are interested in the glucose regulatory system. As a result, we would like to know the exact endogenous production/appearance from the intestine, utilization/degradation and amount of glucose present in every tissue/organ. However, for obvious reason, it is not possible to measure some quantities directly. Consequently, to at least understand some information about the complex dynamics of glucose in the body, we can insert in the body some labeled glucose molecules (the tracer molecules) that will be treated by the body in the exact same way as all the others glucose molecules. Those glucose molecules are built using **isotopic tracers**. An isotope is an atom of the same element with a different number of neutrons and it can be a radioactive or a stable isotope. Here, we will focus on the radioactive ones, since they were used in this study. Radioactive isotopes are not stable atoms and they are turning back in the

original configuration through a process called radioactive decay. This process produces electromagnetic waves that can be detected. Thus, if one creates a glucose molecule with inside one or more radioactive isotopes, it can be detected. This is the case of $[3\ -^3\ H]$ glucose, that contains tritium, the radioactive isotope of hydrogen. The unlabeled glucose is call *tracee*, and the goal of a tracer kinetics study is to infer information about the tracee's kinetics from the tracer's one.
The usual measurement variable of radioactive tracers is the **specific activity (SA)**. It expresses the abundance of a radioactive tracer as follow:

$$SA = \frac{dpm}{mass} \tag{2.1}$$

Where *dpm* are disintegrations per minute, measuring the radioactivity; *mass* is the total mass (tracer + tracee) of the compound. Dpm and mass are measured separately, the first by a scintillation counter, the second by an enzymatic method.

Tracers and model use

As previously said, the goal is to infer from the tracer's kinetics information about the tracee's one, i.e. to measure tracee fluxes, mass and volume from tracer measurements. When dealing with tracer experiments, the data analysis can be performed applying:

- simple formulas;
- non-compartmental model techniques;
- compartmental model approaches.

The three approaches were listed from the simpler to the complex. Increasing complexity is the cost to pay to retrieve more information from the same dataset. Simple formulas calculation is based on two assumptions: the system is homogeneous and both tracer and tracee are in steady state. While the first one may be a plausible simplification that works in some cases, the second one is violated in our experiment, since we are dealing with dynamic data. The non-compartmental model [34] is another common approach used to tackle the problem. Its strength comes from not assuming any model structure regarding the system under study, however, also in this case, it requires that the tracee in steady state. As a result, in our case, a compartmental approach is needed. Furthermore, a model is required to relate the information derived from the gauges taken from the accessible pool (the circulation) with the events taking place in both the accessible and non-accessible parts of the system.

Tracee and Tracer kinetics variables

A scheme of the tracer-tracee system of the experiment can be appreciated in figure 2.2. As mentioned in section 2.1, there were two tracer inputs: a continuous infusion that mimics the endogenous glucose production (EGP), and a component (GIR tracer) proportional to the glucose infusion rate (GIR) that mimics the rate of appearance of an oral glucose challenge in the circulation.
The goal was to estimate EGP. To do so, we used the approach proposed by Steele et al. in 1956 [35]. This method exploits, the tracer-tracee indistinguishably principle, which can be written as:

$$\frac{q(t)}{Q(t)} = \frac{rd(t)}{Rd(t)} = k(t) \tag{2.2}$$

This technique assumes an homogeneous system and it connects tracee unknown kinetics variables to the tracer's ones, since $u(t)$ is known (kinetics variables in equation 2.2 refer to the following figure).

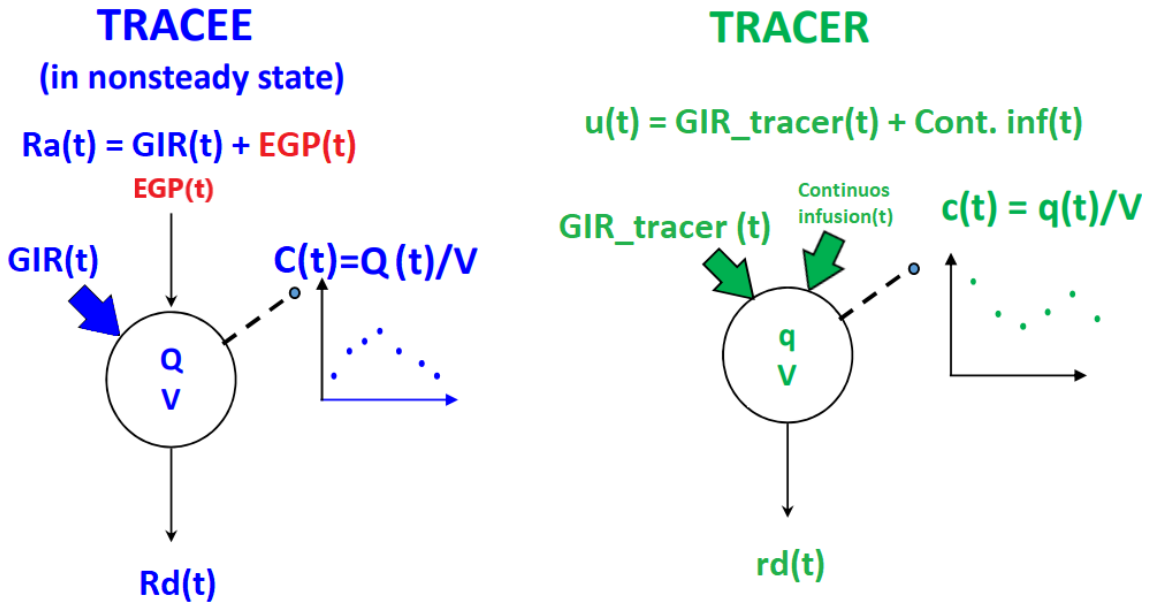

Figure 2.2: Diagram of the tracer-tracee system of the experimental design (sec. 2.1). Glucose is the tracee and $[3{-}^{3}H]$ glucose is the tracer. $C(t)$ is the glucose plasma concentration and $c(t)$ is the tracer plasma concentration. $Q(t)$ and $q(t)$ are the amount of glucose and tracer in the circulation, respectively. V is the volume of the plasma compartment. $Ra(t)$ is the glucose rate of appearance into the circulation, which consists of the infused glucose ($GIR(t)$) and the $EGP(t)$. $u(t)$ is the total infused tracer, which is made up of the continuous infusion ($Cont.inf(t)$) and the infusion proportional to GIR ($GIR\ tracer(t)$). $Rd(t)$ and $rd(t)$ are rates of disappearance from the plasma.

In particular the so called **Steele Equation** calculates the rate of appearance of the tracee as follow:

$$Ra(t) = \frac{u(t)}{ttr(t)} - p \cdot V_{tot} \cdot C(t) \cdot \frac{\dot{ttr}(t)}{ttr(t)} \tag{2.3}$$

Where *ttr(t)* is the tracer/tracee ratio and it is the most convenient way to express tracer data. V_{tot} is the total volume of distribution of glucose. Since the Steele equation requires the volume of the accessible compartment, it is estimated as a fraction of the total volume of distribution, via the pool fraction p. In radioactive tracers, the specific activity (SA) almost coincides with ttr, in fact:

$$SA(t) = \frac{q(t)}{Q(t) + q(t)} \approx \frac{q(t)}{Q(t)} = ttr(t) \tag{2.4}$$

where $Q(t)$ is the mass of the unlabelled compound and $q(t)$ is the mass of the tracer, that is negligible, compared to $Q(t)$ in case of a radioactive tracer. Consequently, equation 2.3 can be written as:

$$Ra(t) = \frac{u(t)}{SA(t)} - p \cdot V_{tot} \cdot C(t) \cdot \frac{\dot{SA}(t)}{SA(t)} \tag{2.5}$$

An important remark is that if $\dot{SA}(t) = 0$, the Steele Equation reduces to the steady state formula:

$$Ra(t) = \frac{u(t)}{SA(t)} \tag{2.6}$$

That is the formulation that can be obtained applying the "simple formula approach" when both tracee and tracer are in steady state. This is a desirable scenario since $p \cdot V_{tot} \cdot C(t) \cdot \frac{\dot{SA}(t)}{SA(t)}$, which accounts for the non-steady state error, depends on the chosen model. In fact, it can be proven that the estimation of *Ra(t)* is model dependent. Using other approaches, like the **Radziuk Equation** [36], will produce a different estimation of the tracee rate of apperance (if $\dot{SA}(t)$ is not equal to zero).

The Tracer-to-Tracee Clamp Technique

A possible solution to tackle the model dependency of the calculation of *Ra(t)* is to infuse the tracer so that the non-stready state error is minimized. To do so, we can exploit expectations on EGP profile. It is known that after a meal, plasma glucose increases, and its production by the liver is suppressed. That's why, the

continuous tracer infusion was reduced when the "meal" infusion started (see figure 2.1). Ideally, if the tracer is properly infused, the non-steady state error becomes close to zero and the estimation of the rate of appearance is model independent.

When *Ra(t)* is calculated, the endogenous glucose production can be simply calculated by subtraction (equation 2.7), since the glucose infusion rate in input is known.

$$EGP(t) = Ra(t) - GIR(t) \tag{2.7}$$

In figure 2.3, the estimated EGP is depicted. On average, in the S occasion, EGP is more suppressed in the first part of the experiment compared to the NS occasion. This is reasonable since glucagon is suppressed from $t = 0$ *[min]* to $t = 120$ *[min]* in the S experiment. The following infusion of glucagon produces a rise in EGP that is clearly present in the S occasion and absent at all in the NS one. Variability of EGP (std) remains almost constant in NS, instead it increases around the peak after EGP rise in S. This is also reasonable since subjects received different insulin infusion, and it is known that insulin has an influence on glucagon action on EGP (see section 1.1). In both occasions EGP doesn't come back to basal at the end of the experiment (on average).

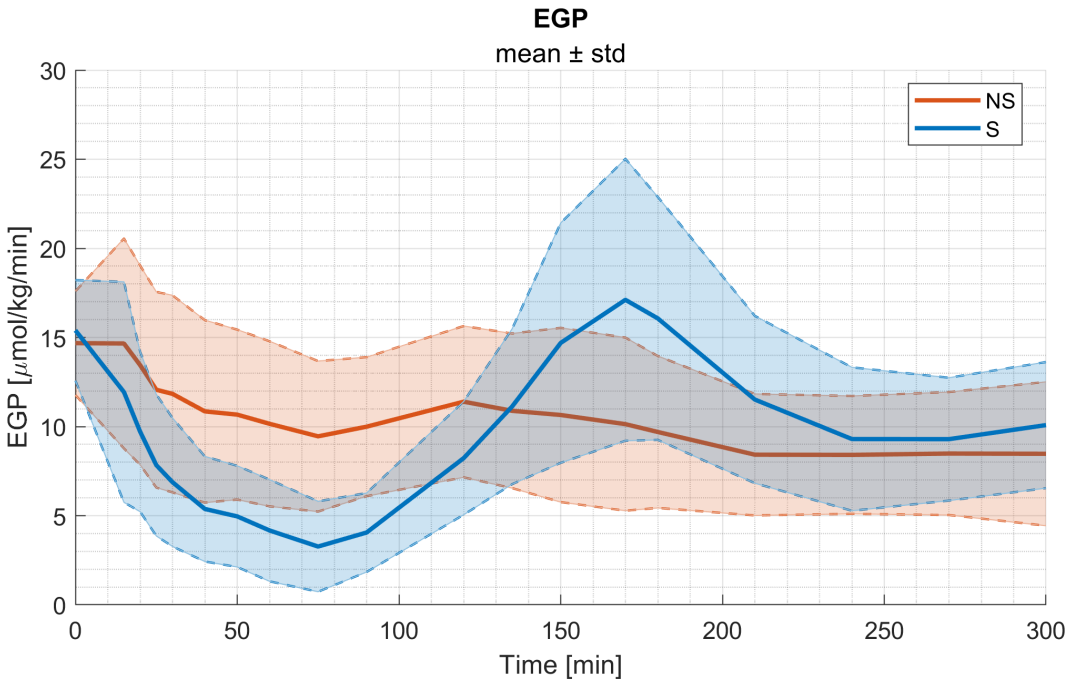

Figure 2.3: Estimated EGP using Steele equation.

In figure 2.4 a comparison of EGP in the 3 insulin groups is reported. Firstly, dif-

ferences between the two occasions are similar to the average ones in all the groups. It is clear that different insulin infusions have a different impact on EGP. In particular, in the NS experiment average EGP profile decreases with increasing insulin infusion. This confirmed that glucose production inhibition by insulin is proportional to insulin concentration. Also in the S occasion this effect is present, especially comparing group with severely impaired insulin secretion (0.6 Ins) with normal insulin secretion group (1.0 Ins) in the first part of the experiment, when glucagon is suppressed. Moreover, also the relationship between glucagon and insulin profiles can be investigated. Comparing the mean EGP in S vs NS in each group, a smaller difference in the mean profiles is present with increased insulin level. Consequently, data suggests a reduction of glucagon action on EGP when insulin concentration is higher. A final remark concerns the EGP variability (standard deviation) in *1.0 Ins group* with respect to the others in the S scenario. Especially after glucagon infusion at $t = 120$ *[min]*, an higher variability is present in this group that may suggest that higher insulin concentrations have an increased action variability on hepatic glucagon sensitivity.

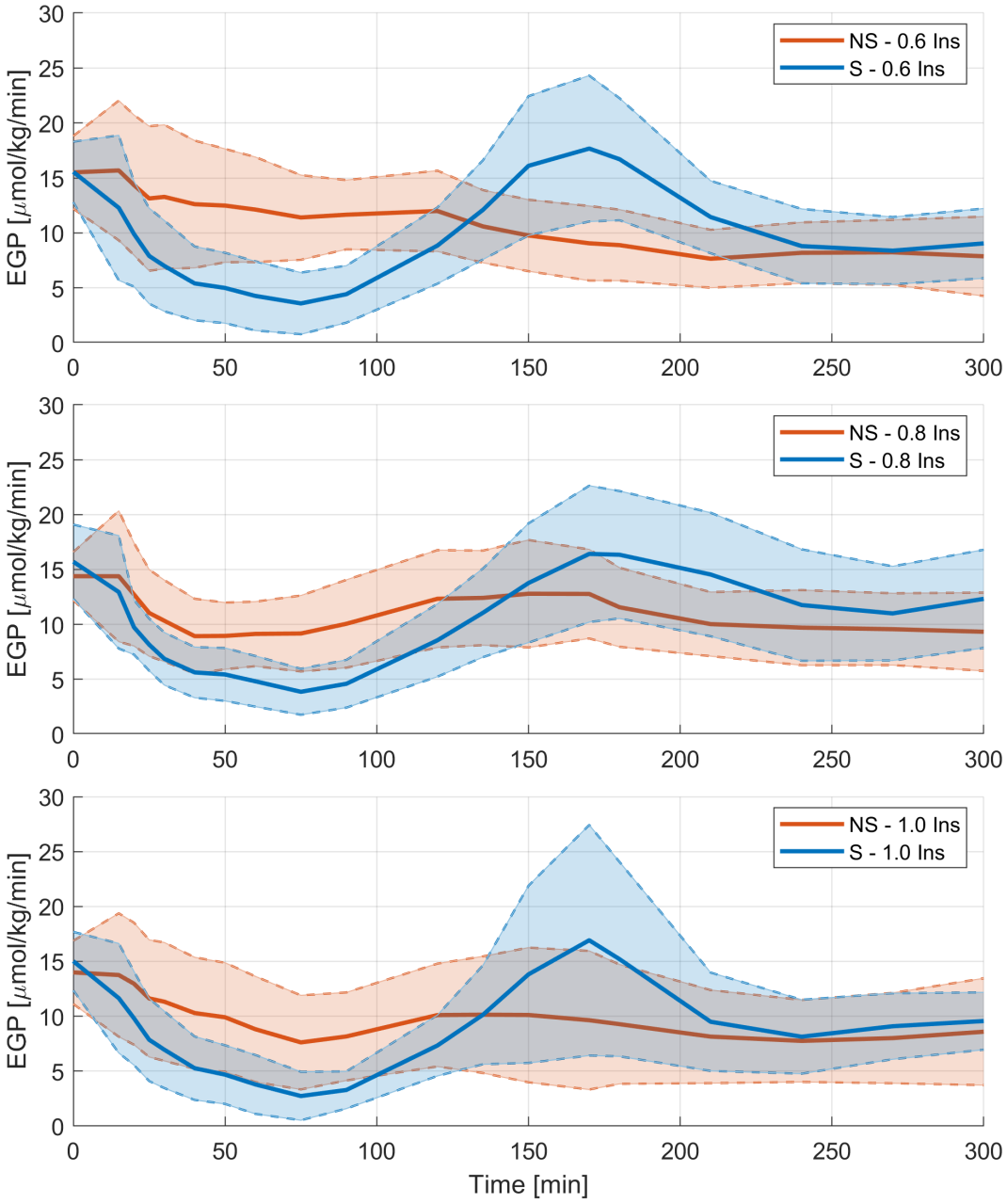

Figure 2.4: Comparison of EGP in the 3 groups respect to the infused insulin level.

2.2.1 Smoothing of the specific activity

As seen in the previous section, the first step to estimate EGP is to calculate the specific activity, as the ratio between the tracer concentration and the glucose concentration. Ideally, SA should remain constant during all the study; however, this is not true in clinical practice, even if the tracer is infused in a way that mimic the expected tracee profile. Thus, there is the need to correct from the non-steady state error, and

the derivative of SA must be calculated. Moreover, due to several sources of noise (from the measurement devices to the actual measurement process, like sampling from the test tube), a smoothing process of the raw specific activity is necessary.
The numerical differentiation of digitized signals is not a trivial step, simple approaches can lead to unsatisfying results, in particular regarding the noise amplification introduced by the differentiation operation. Indeed, it is referable to a filtering procedure with an high-pass filter; since the measurement noise is assumed as a white noise with a known variance, the differentiation process will amplify it. **Deconvolution** can be a good approach to perform the derivative step, and it has also the plus of solving our second need, the smoothing of SA (for more details, see Appendix A).

Use of deconvolution in this study

As previously mentioned, the goal of this pre-processing step is to smooth the specific activity and calculate its derivative. Using the same notation of Appendix A, the derivative of SA is *u(k)* and SA data points are *y(k)*; *k* is the k-th measurement, since we assume to work in a discrete time domain. The transfer matrix of the system is a simple first order integrator, since we would like to calculate the derivative of the output signal. Moving into the frequency domain through a Z-transform, the system transfer function can be formalized as:

$$H(z) = \frac{1}{1 - z^{-1}} \tag{2.8}$$

Derivative of SA was estimated with the Bayesian approach described in the Appendix and γ was selected exploiting the third consistent criterion. The smoothed version of SA is the result of a re-convolution process using the estimated input.
In figure 2.5 the smoothing and differentiation of SA in a representative subject is shown. Besides the value of the regularization parameter γ, also a metric that describes the amount of regularization is included (*q/n*). It could take values between zero and one. Zero means that it was not applied a regularization of the estimated signal (the same of using the least square approach), instead a value of 1 means that the estimation process was based only on prior information on *u(k)*. This metric was developed since γ is highly dependent on different factors and its value does not reflect how much the estimated signal was regularized. Finally it is worth noting that a virtual and more dense (with respect to the sampling one) time grid was used.

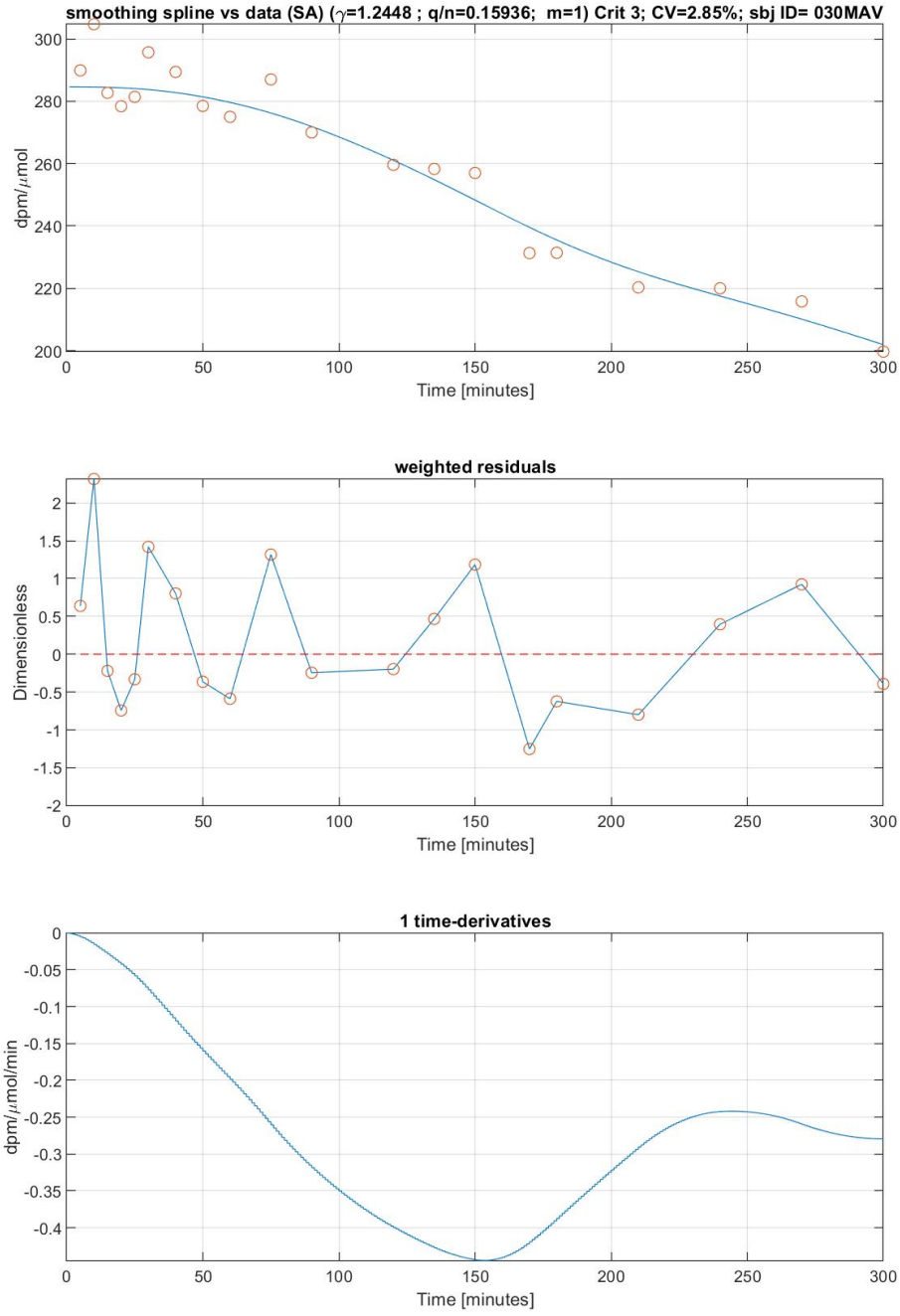

Figure 2.5: Smoothing process of specific activity (SA) with deconvolution in the not suppressed occasion in a representative subject. First panel: data (red circles) and smooth version (blu line) of SA. Second panel: weighted residuals of the reconvoluted output. Third panel: estimated derivative of SA.

2.3 Estimation error on EGP

As highlighted in section 2.2, EGP estimation is the result of a cascade of calculations. Thus, propagation of error to estimate EGP's error of measurement (v) is cumbersome. Consequently, here we made a reasonable assumption about the variance of each element of v (since it is assumed gaussian), based on the resulting coefficient of variation. It is also important to remember that the estimation of EGP is model dependent, only if SA remains constant during all the experiment a non-steady state correction is not needed and the dependency vanishes. However, this is not what happens in real experiments. The non-steady state correction will be higher when the absolute value of the derivative of SA is significantly greater than zero (eq. 2.5). In such time instants there is the greater model dependency of EGP estimates. These time points can be considered the EGP values with more uncertainty. Therefore, we embedded this information inside the model of EGP's error of measurement as follow:

$$std_v(k) = std_b + \delta \dot{SA}(k), \qquad \delta = \frac{std_b}{max(|\dot{SA}|)} \tag{2.9}$$

Where $std_{EGP}(k)$ is the standard deviation (std) of the measurement error for the k-th samples, $v(k)$. std_b is the std value of time points where SA was almost constant (where there is no need of non-steady state correction and EGP's estimates are not dependent from the selected model). The additional part, $\delta \dot{SA}(k)$, increases EGP uncertainty with respect to the derivative of SA. δ was set to have a maximum std double with respect to the basal value in case of maximum absolute value of SA derivative.

In figure 2.6 and figure 2.7, SA data vs smoothed SA and corresponding EGP estimated using Steele equation are displayed for two illustrative subjects. In both subjects SA showed some variation during the experiment in S and NS occasions. Thus, EGP's estimates corresponding to those time points where SA had the greatest variation will have an higher uncertainty.

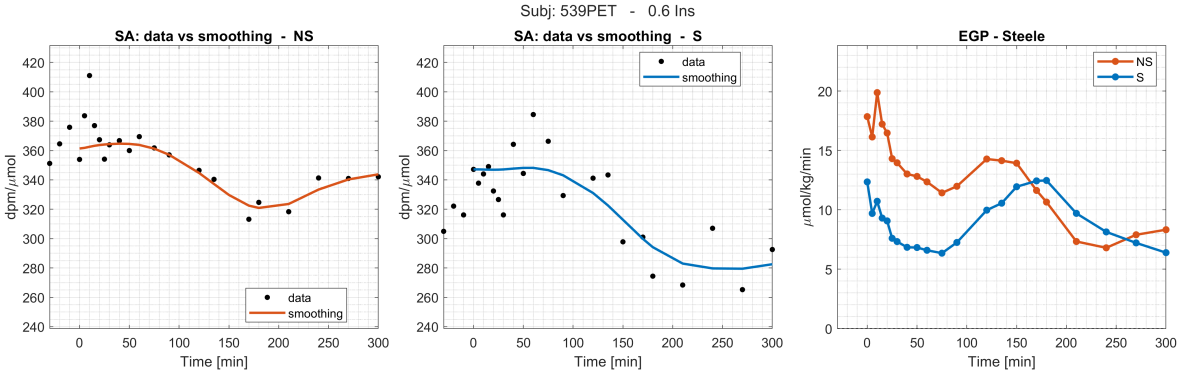

Figure 2.6: Smoothing of SA and EGP estimation using Steele equation for subject 539PET in both suppressed (S) and not suppressed (NS) occasion.

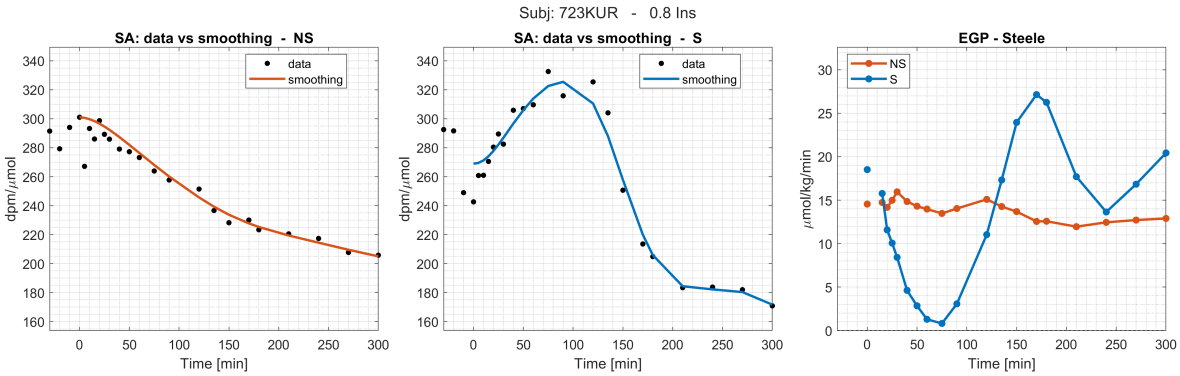

Figure 2.7: Smoothing of SA and EGP estimation using Steele equation for subject 723KUR in both suppressed (S) and not suppressed (NS) occasion.

An important comment concerns the correlation among EGP estimates. As seen before, EGP is estimated using Steele equation (eq.2.5). Thus, there is the need of smoothing SA and calculated its derivative (section 2.2.1). Consequently, each EGP's estimate is not based only on data collected in a single time point, rather it is influenced by measurements taken at different time instants. As a result, **EGP's error should not be considered uncorrelated**. During model assessment, in particular within the residual analysis step, this remark must be considered.

3 Models

3.1 Linear models of EGP

In this section, all the tested linear models of EGP are presented. In these models, EGP is described as a linear combination of different factors that are proportional to the measured signals (glucose, insulin and glucagon) or their delayed actions, or their rate of change.

3.1.1 Model 1

The first model is the model proposed by Dalla Man et al. in 2008 (model 6 in the original paper) [25]. It was built with the aim to measure hepatic insulin sensitivity and is essentially an improved version of the EGP description that can be derived from the so called *minimal model* [21], one of the pioneer models in this research field. Model equation are:

$$\begin{cases} EGP(t) = k_{p1} - k_{p2} \cdot G(t) - k_{p3} \cdot X^L(t) - k_{p7} \cdot G^{Der}(t) \\ \dot{X^I}(t) = -k_{p5} \cdot [X^I(t) - I(t)] & X^I(0) = I_b \\ \dot{X^L}(t) = -k_{p5} \cdot [X^L(t) - X^I(t)] & X^L(0) = I_b \\ G^{Der}(t) = \begin{cases} \frac{\partial G(t)}{\partial t} & if \ \ \frac{\partial G(t)}{\partial t} \geq 0 \\ 0 & if \ \ \frac{\partial G(t)}{\partial t} < 0 \end{cases} \\ k_{p1} = EGP_b + k_{p2} \cdot G_b + k_{p3} \cdot X^L(0) \end{cases} \tag{3.1}$$

where $G(t)$ $[mmol/l]$ is glucose plasma concentration, $I(t)$ $[pmol/l]$ is insulin plasma concentration and $G^{Der}(t)$ $[mmol/l/min]$ is glucose rate of change, $X^I(t)$ $[pmol/l]$ is a delayed insulin signal and $X^L(t)$ $[pmol/l]$ is a further delayed insulin profile. k_{p2} $[ml/Kg/min]$ is the glucose sensitivity of the liver,
k_{p3} $[(\mu mol/Kg/min)/(pmol/l)]$ is hepatic insulin sensitivity , k_{p7} $[ml/Kg]$ describes the magnitude of the glucose rate of change action on EGP, k_{p5} $[1/min]$ is the insulin transfer coefficient and it describes how fast is insulin action dynamics. The part of the model proportional to glucose and its rate of change $(k_{p2} \cdot G(t) + k_{p7} \cdot G^{Der}(t))$ can be related to the above-basal insulin secretion, occurring after a meal [37], that is a surrogate of the portal insulin signal [38]. Finally, k_{p1} $[\mu mol/kg/min]$ is a parameter function of the others, used as offset for the basal state (equilibrium and also initial state).

3.1.2 Model 2

The second tested model is the EGP description presented inside the FDA approved "UVA/PADOVA type I diabetes simulator" [39]. The model equations are:

$$\begin{cases} EGP(t) = k_{p1} - k_{p2} \cdot G(t) - k_{p3} \cdot X^L(t) + k_{p4} \cdot X^{Gn}(t) \\ \dot{X^I}(t) = -k_{p5} \cdot [X^I(t) - I(t)] & X^I(0) = I_b \\ \dot{X^L}(t) = -k_{p5} \cdot [X^L(t) - X^I(t)] & X^L(0) = I_b \\ \dot{X^{Gn}}(t) = -k_{p6} \cdot [X^{Gn}(t) - Gn(t)] & X^{Gn}(0) = Gn_b \\ k_{p1} = EGP_b + k_{p2} \cdot G_b + k_{p3} \cdot X^L(0) - k_{p4} \cdot X^{Gn}(0) \end{cases} \tag{3.2}$$

With respect to the previous model, here the glucose rate of change is not present. Instead, EGP is stimulated by a glucagon plasma concentration $Gn(t)$ $[pmol/l]$ with some delay $X^{Gn}(t)$ $[pmol/l]$. Thus, k_{p4} $[(\mu mol/kg/min)/(pmol/l)]$ is the hepatic glucagon sensitivity and k_{p6} $[1/min]$ is the glucagon transfer coefficient.

3.1.3 Model 3

This model in equal to model 2 with a component that takes into consideration the glucagon "evanescent" effect ([40],[26]). This effect (E) is described as an hyperbolic tangent function, as previously suggested [12]. This is not a structural model estimated with an ad hoc protocol, since, from the best of our knowledge, such a model is not present in the literature. The formulation of the evanescent effect of

this model considers a fall in glucagon action on EGP even if glucagon concentration remains above basal. These are the model equations:

$$\begin{cases} EGP(t) = k_{p1} - k_{p2} \cdot G(t) - k_{p3} \cdot X^L(t) + k_{p4} \cdot X^{Gne}(t) \\ \dot{X^I}(t) = -k_{p5} \cdot [X^I(t) - I(t)] & X^I(0) = I_b \\ \dot{X^L}(t) = -k_{p5} \cdot [X^L(t) - X^I(t)] & X^L(0) = I_b \\ \dot{X^{Gn}}(t) = -k_{p6} \cdot [X^{Gn}(t) - Gn(t)] & X^{Gn}(0) = Gn_b \\ X^{Gne}(t) = \begin{cases} X^{Gn}(t) & if \quad t < t_i \\ X^{Gn}(t) \cdot E(t) & if \quad t \geq t_i \end{cases} & X^{Gne}(0) = Gn_b \\ E(t) = \frac{1}{2} \cdot [1 - tanh(\frac{t-t_0}{\tau})] \\ k_{p1} = EGP_b + k_{p2} \cdot G_b + k_{p3} \cdot X^L(0) - k_{p4} \cdot X^{Gne}(0) \end{cases} \tag{3.3}$$

where $k_{p4} \cdot X^{Gne}(t)$ is the glucagon action incorporating the evanescence effect and t_i $[min]$ represented the time at which the glucagon infusion starts. In the not-suppressed occasion it is equal to 0 [min], instead in the suppressed one is equal to 120 [min]. Before this moment, no evanescent effect is considered on glucagon action. Parameter t_0 $[min]$ is the time instant where the glucagon action is reduced by 50% respect to its value without the evanescence effect and τ $[min]$ models the shape of the hyperbolic tangent, the smaller it is, the faster the fall (figure 3.1). t_0 and τ are new model parameters that will be estimated from the data.

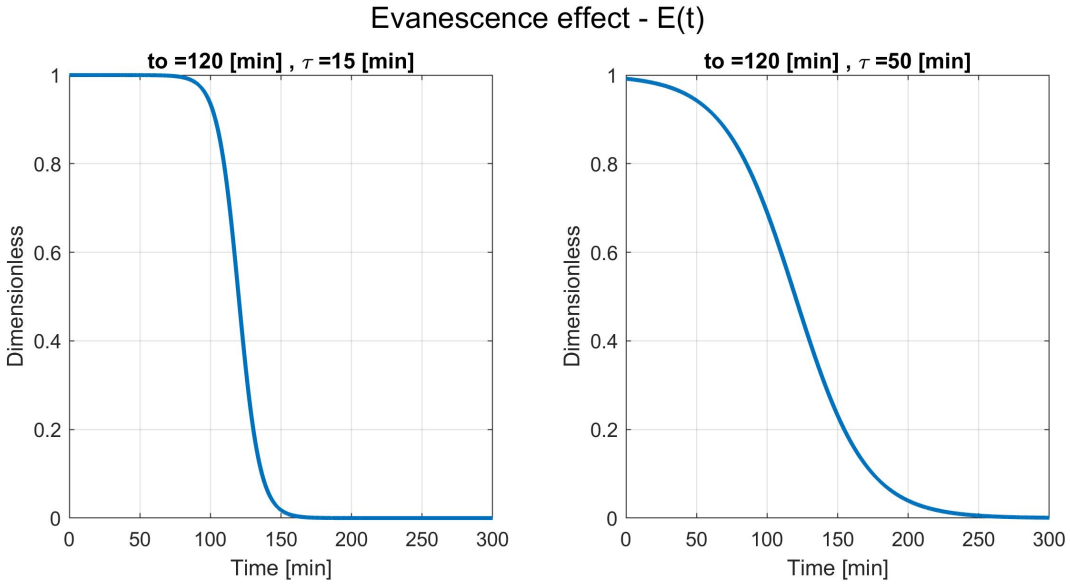

Figure 3.1: Model of glucagon evanescence effect, E(t). Comparison of E profile with two different τ values. t_i is fixed to t = 0 [min].

3.1.4 Model 4

The only difference with respect the previous model is that glucagon action on EGP is directly proportional to glucagon concentrations instead of his delayed version. Thus, model 4 has one parameter less respect to model 3.

$$\begin{cases} EGP(t) = k_{p1} - k_{p2} \cdot G(t) - k_{p3} \cdot X^L(t) + k_{p4} \cdot X^{Gne}(t) \\ \dot{X^I}(t) = -k_{p5} \cdot [X^I(t) - I(t)] & X^I(0) = I_b \\ \dot{X^L}(t) = -k_{p5} \cdot [X^L(t) - X^I(t)] & X^L(0) = I_b \\ X^{Gne}(t) = \begin{cases} Gn(t) & if \quad t < t_i \\ Gn(t) \cdot E(t) & if \quad t \geq t_i \end{cases} & X^{Gne}(0) = Gn_b \\ E(t) = \frac{1}{2} \cdot [1 - tanh(\frac{t-t_0}{\tau})] \\ k_{p1} = EGP_b + k_{p2} \cdot G_b + k_{p3} \cdot X^L(0) - k_{p4} \cdot X^{Gne}(0) \end{cases} \tag{3.4}$$

3.1.5 Model 5

In this model, the action of glucose rate of change on EGP ($k_{p7} \cdot G^{Der}(t)$) is reintroduced. The remaining part of the model is the same of model 3 (eq. 3.3).

$$\begin{cases} EGP(t) = k_{p1} - k_{p2} \cdot G(t) - k_{p3} \cdot X^L(t) + k_{p4} \cdot X^{Gne}(t) - k_{p7} \cdot G^{Der}(t) \\ \dot{X^I}(t) = -k_{p5} \cdot [X^I(t) - I(t)] & X^I(0) = I_b \\ \dot{X^L}(t) = -k_{p5} \cdot [X^L(t) - X^I(t)] & X^L(0) = I_b \\ \dot{X^{Gn}}(t) = -k_{p6} \cdot [X^{Gn}(t) - Gn(t)] & X^{Gn}(0) = Gn_b \\ X^{Gne}(t) = \begin{cases} X^{Gn}(t) & if \quad t < t_i \\ X^{Gn}(t) \cdot E(t) & if \quad t \geq t_i \end{cases} & X^{Gne}(0) = Gn_b \\ E(t) = \frac{1}{2} \cdot [1 - tanh(\frac{t-t_0}{\tau})] \\ G^{Der}(t) = \begin{cases} \frac{\partial G(t)}{\partial t} & if \quad \frac{\partial G(t)}{\partial t} \geq 0 \\ 0 & if \quad \frac{\partial G(t)}{\partial t} < 0 \end{cases} \\ k_{p1} = EGP_b + k_{p2} \cdot G_b + k_{p3} \cdot X^L(0) - k_{p4} \cdot X^{Gne}(0) \end{cases} \tag{3.5}$$

3.1.6 Model 6

With respect to model 5 (eq. 3.5), in this model glucagon exerts its action without delay. That's why, model 6 has one parameter less with respect to model 5.

$$\begin{cases} EGP(t) = k_{p1} - k_{p2} \cdot G(t) - k_{p3} \cdot X^L(t) + k_{p4} \cdot X^{Gne}(t) - k_{p7} \cdot G^{Der}(t) \\ \dot{X^I}(t) = -k_{p5} \cdot [X^I(t) - I(t)] \qquad X^I(0) = I_b \\ \dot{X^L}(t) = -k_{p5} \cdot [X^L(t) - X^I(t)] \qquad X^L(0) = I_b \\ X^{Gne}(t) = \begin{cases} Gn(t) & if \quad t < t_i \\ Gn(t) \cdot E(t) & if \quad t \geq t_i \end{cases} \qquad X^{Gne}(0) = Gn_b \\ E(t) = \frac{1}{2} \cdot [1 - tanh(\frac{t-t_0}{\tau})] \\ G^{Der}(t) = \begin{cases} \frac{\partial G(t)}{\partial t} & if \quad \frac{\partial G(t)}{\partial t} \geq 0 \\ 0 & if \quad \frac{\partial G(t)}{\partial t} < 0 \end{cases} \\ k_{p1} = EGP_b + k_{p2} \cdot G_b + k_{p3} \cdot X^L(0) - k_{p4} \cdot X^{Gne}(0) \end{cases} \tag{3.6}$$

3.1.7 Model 7

This model is an evolution of model 3 (eq. 3.3) that takes into consideration also glucagon rate of change through parameter $k_{p8}[(\mu mol/kg)/(pmol/l)]$.

$$\begin{cases} EGP(t) = k_{p1} - k_{p2} \cdot G(t) - k_{p3} \cdot X^L(t) + k_{p4} \cdot X^{Gne}(t) + k_{p8} \cdot Gn^{Der}(t) \\ \dot{X^I}(t) = -k_{p5} \cdot [X^I(t) - I(t)] \qquad X^I(0) = I_b \\ \dot{X^L}(t) = -k_{p5} \cdot [X^L(t) - X^I(t)] \qquad X^L(0) = I_b \\ \dot{X^{Gn}}(t) = -k_{p6} \cdot [X^{Gn}(t) - Gn(t)] \qquad X^{Gn}(0) = Gn_b \\ X^{Gne}(t) = \begin{cases} X^{Gn}(t) & if \quad t < t_i \\ X^{Gn}(t) \cdot E(t) & if \quad t \geq t_i \end{cases} \qquad X^{Gne}(0) = Gn_b \\ E(t) = \frac{1}{2} \cdot [1 - tanh(\frac{t-t_0}{\tau})] \\ Gn^{Der}(t) = \begin{cases} \frac{\partial Gn(t)}{\partial t} & if \quad \frac{\partial Gn(t)}{\partial t} \geq 0 \\ 0 & if \quad \frac{\partial Gn(t)}{\partial t} < 0 \end{cases} \\ k_{p1} = EGP_b + k_{p2} \cdot G_b + k_{p3} \cdot X^L(0) - k_{p4} \cdot X^{Gne}(0) \end{cases} \tag{3.7}$$

After a comparison of nine published or new EGP models, Emami et al. in 2017

[26] showed that glucagon rate of change was important to achieved the best fit. In fact, glucagon derivative can be helpful to model an hepatic response to a rapid increase of plasma glucagon concentration.

3.1.8 Model 8

Model 8 is the most complex linear model tested in this thesis. It combines all the different parts of the previous models. So, it considers both glucose and glucagon rate of change and glucagon evanescence effect is present and assumes that glucagon exerts its action with some delay.

$$
\begin{cases}
EGP(t) = k_{p1} - k_{p2} \cdot G(t) - k_{p3} \cdot X^L(t) + k_{p4} \cdot X^{Gne}(t) - k_{p7} \cdot G^{Der}(t) + k_{p8} \cdot Gn^{Der}(t) \\
\dot{X^I}(t) = -k_{p5} \cdot [X^I(t) - I(t)] \qquad X^I(0) = I_b \\
\dot{X^L}(t) = -k_{p5} \cdot [X^L(t) - X^I(t)] \qquad X^L(0) = I_b \\
\dot{X^{Gn}}(t) = -k_{p6} \cdot [X^{Gn}(t) - Gn(t)] \qquad X^{Gn}(0) = Gn_b \\
X^{Gne}(t) = \begin{cases} X^{Gn}(t) & if \quad t < t_i \\ X^{Gn}(t) \cdot E(t) & if \quad t \geq t_i \end{cases} \qquad X^{Gne}(0) = Gn_b \\
E(t) = \frac{1}{2} \cdot [1 - tanh(\frac{t - t_0}{\tau})] \\
G^{Der}(t) = \begin{cases} \frac{\partial G(t)}{\partial t} & if \quad \frac{\partial G(t)}{\partial t} \geq 0 \\ 0 & if \quad \frac{\partial G(t)}{\partial t} < 0 \end{cases} \\
Gn^{Der}(t) = \begin{cases} \frac{\partial Gn(t)}{\partial t} & if \quad \frac{\partial Gn(t)}{\partial t} \geq 0 \\ 0 & if \quad \frac{\partial Gn(t)}{\partial t} < 0 \end{cases} \\
k_{p1} = EGP_b + k_{p2} \cdot G_b + k_{p3} \cdot X^L(0) - k_{p4} \cdot X^{Gne}(0)
\end{cases}
\tag{3.8}
$$

3.2 Non linear models of EGP

As seen in the physiology section 1.1, insulin level modulates the hepatic response to glucagon. Therefore, a non linear relationship between glucagon and insulin should be tested. In literature, this relationship is model in several ways, and a multiplicative description seems to be the most suitable to describe this phenomenon ([41],[26]). In this section, we will present four EGP model structures that investigate different possible non linear interactions.

3.2.1 Non linear model 1

The first non linear model takes into consideration the same dynamics of the linear model 3 (eq. 3.3) for insulin and glucagon. When all the input signals (glucose, insulin and glucagon) are in basal state, EGP is not perturbed and it is equal to its basal rate EGP_b $[\mu mol/kg/min]$. If glucagon remains in basal state ($Gn(t) = Gn_b$), EGP is proportional to the above basal glucose concentration through parameter α_1 $[ml/Kg/min]$ and to insulin delayed profile ($X^L(t)$) through parameter β_1 $[(\mu mol/kg/min)/(pmol/l)]$. However, when glucagon is not in basal state, it will influence both glucose and delayed insulin actions on EGP, through parameter α_2 $[l/pmol]$ and β_2 $[l/pmol]$ respectively; reducing their inhibition effect. The model equations are:

$$\begin{cases} EGP(t) = EGP_b - \frac{\alpha_1}{1+\alpha_2 \cdot X^{Gn}(t)} \cdot (G(t) - G_b) - \frac{\beta_1}{1+\beta_2 \cdot X^{Gn}(t)} \cdot X^L(t) \\ \dot{X^I}(t) = -k_{p5} \cdot [X^I(t) - (I(t) - I_b)] \qquad X^I(0) = 0 \\ \dot{X^L}(t) = -k_{p5} \cdot [X^L(t) - X^I(t)] \qquad X^L(0) = 0 \\ \dot{X^{Gn}}(t) = -k_{p6} \cdot [X^{Gn}(t) - (Gn(t) - Gn_b)] \quad X^{Gn}(0) = 0 \end{cases} \tag{3.9}$$

3.2.2 Non linear model 2

With respect to non linear model 1, in this model glucagon modulation has an effect only on delayed insulin action on EGP ($X^L(t)$); since it seems that glucose level is not in relation with glucagon action [42].

$$\begin{cases} EGP(t) = EGP_b - \alpha_1 \cdot (G(t) - G_b) - \frac{\beta_1}{1+\beta_2 \cdot X^{Gn}(t)} \cdot X^L(t) \\ \dot{X^I}(t) = -k_{p5} \cdot [X^I(t) - (I(t) - I_b)] \qquad X^I(0) = 0 \\ \dot{X^L}(t) = -k_{p5} \cdot [X^L(t) - X^I(t)] \qquad X^L(0) = 0 \\ \dot{X^{Gn}}(t) = -k_{p6} \cdot [X^{Gn}(t) - (Gn(t) - Gn_b)] \quad X^{Gn}(0) = 0 \end{cases} \tag{3.10}$$

3.2.3 Non linear model 3

Non linear model 3 still has a multiplicative relationship between glucagon and insulin. However, in this case it is delayed insulin ($X^L(t)$) that modulates delayed glucagon action ($X^{Gn}(t)$) on EGP (in the previous two models, it was the reverse); this is based on the hypothesis that high insulin level reduces hepatic stimulation effect of glucagon, as reported in the physiology section 1.1.

$$\begin{cases} EGP(t) = EGP_b - \alpha_1 \cdot (G(t) - G_b) + \frac{\beta_1}{1+\beta_2 \cdot X^L(t)} \cdot X^{Gn}(t) \\ \dot{X^I}(t) = -k_{p5} \cdot [X^I(t) - (I(t) - I_b)] & X^I(0) = 0 \\ \dot{X^L}(t) = -k_{p5} \cdot [X^L(t) - X^I(t)] & X^L(0) = 0 \\ \dot{X^{Gn}}(t) = -k_{p6} \cdot [X^{Gn}(t) - (Gn(t) - Gn_b)] & X^{Gn}(0) = 0 \end{cases} \tag{3.11}$$

3.2.4 Non linear model 4

Non linear model 4 has the same structure of non linear model 3 (eq.3.12), with the addition of a component proportional to glucagon rate of change through parameter γ $[(\mu mol/kg)/(pmol/l)]$. Since, as explained for the linear model 7 (eq. 3.7), it may help to better describe a rapid EGP increase.

$$\begin{cases} EGP(t) = EGP_b - \alpha_1 \cdot (G(t) - G_b) + \frac{\beta_1}{1+\beta_2 \cdot X^L(t)} \cdot X^{Gn}(t) + \gamma \cdot Gn^{Der}(t) \\ \dot{X^I}(t) = -k_{p5} \cdot [X^I(t) - (I(t) - I_b)] & X^I(0) = 0 \\ \dot{X^L}(t) = -k_{p5} \cdot [X^L(t) - X^I(t)] & X^L(0) = 0 \\ \dot{X^{Gn}}(t) = -k_{p6} \cdot [X^{Gn}(t) - (Gn(t) - Gn_b)] & X^{Gn}(0) = 0 \\ Gn^{Der}(t) = \begin{cases} \frac{\partial Gn(t)}{\partial t} & if \ \ \frac{\partial Gn(t)}{\partial t} \geq 0 \\ 0 & if \ \ \frac{\partial Gn(t)}{\partial t} < 0 \end{cases} \end{cases} \tag{3.12}$$

4

Model Identification and Assessment

4.1 Model identification

In this section, we will introduce the model identification process and its application in this thesis. The theory behind is huge, thus here we will just summarize the main steps and approaches. For a detailed and formal explanation see chapter 6 of *Introduction to Modeling in Physiology and Medicine, Cobelli C.,Carson E.* [43].

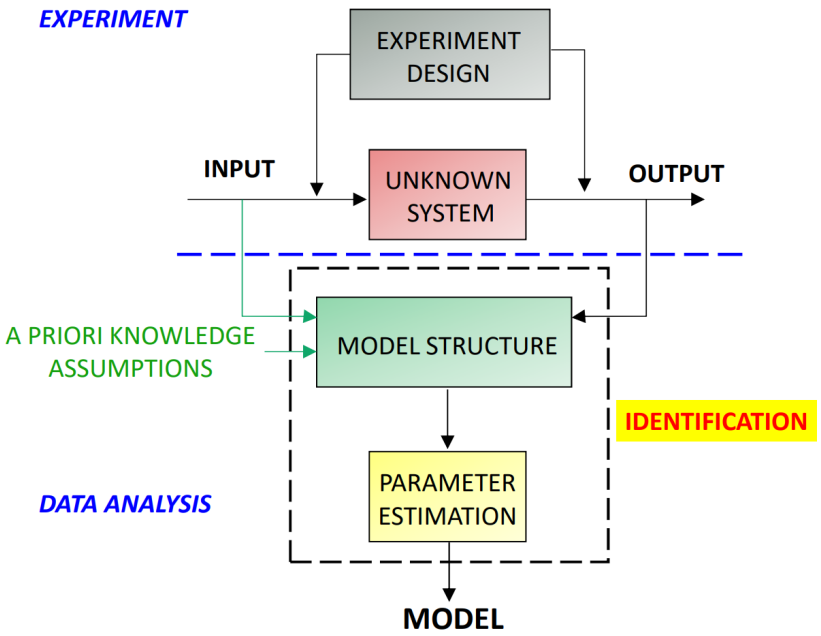

Figure 4.1: Diagram of overall modeling identification procedure. Credit: Chiara Dalla Man.

Modeling is the realization of a mathematical description (the model) of an analyzed system. To do so, firstly you need a model structure, such as the ones in section 3.1 for EGP. These models are parametric models, that is, there is a set of parameters p appearing in model equations that is initially unknown. The goal of the following techniques is assigning numerical values to p exploiting the information about the system (measuring its output) after an input-output experiment, where the input is known (figure 4.1).

4.1.1 A PRIORI IDENTIFIABILITY

Before trying to estimate the unknown parameter values, it is fundamental to verify if the collected measurements contain enough information to uniquely estimate all the parameters of the proposed model structure. In literature, this problem is called *a priori* or *structural identifiability problem*. Addressing this issue (that is posed under the ideal condition of noise–free observable variables, error–free model structure and continuous–time measurements), it become clear whether one or more parameters are not identifiable from the data. If so, a simpler model structure must be formulated.

If the proposed model is time invariant and has a linear kinetics (thus, it can be expressed as in eq. 4.1) the *a priori* identifiability problem can be tackled with the **Transfer Function Method**.

$$\begin{cases} \dot{x(t)} &= F(p) \cdot x(t) + G(p) \cdot u(t) \\ y(t) &= H(p) \cdot x(t) + J(p) \cdot u(t), \qquad\qquad x(0) = x_0 \end{cases} \tag{4.1}$$

where $x(t)$ is the r-dimensional state vector, $u(t)$ is the q-dimensional input vector and $y(t)$ is the n-dimensional measurement vector (output of the system). F, G, H, J are time-invariant matrices that contain the model's parameters (m-dimensional vector p). This method exploits the Laplace transform to calculate the transfer function matrix of the system $H(s)$, for each input-output pair. Such matrices are rational functions (a ratio between two polynomials). The polynomials' parameters (vector ϕ), called observable parameters, can be expressed in function of the model's parameters ($\phi = f(p)$). Thus a set of equations, called *exhaustive summary*, that connects the two vectors can be written. If it is possible to uniquely solving the system respect to p, the model is *a priori globally* identifiable. If a set of finite solutions exists, the model is *a priori locally* identifiable. When the exhaustive summary solved respect to p admits infinite solutions, the model is *a priori* not identifiable.

If the proposed model structure has a non linear dynamics or is time-variant, the transfer function method cannot be used. A suitable alternative is the **Taylor Series Expansion Method**. For sake of simplicity, let us consider a system with one measurement variable y. The Taylor series expansion of y in t^* is:

$$y(p,t) = y(p,t^*) + (t-t^*)\dot{y}(p,t^*) + \frac{(t-t^*)^2}{2!}\ddot{y}(p,t^*) + \frac{(t-t^*)^3}{3!}\dddot{y}(\mathbf{p},t^*) + \ldots \tag{4.2}$$

where $y(p,t^*), \dot{y}(p,t^*), \ddot{y}(p,t^*), \dddot{y}(p,t^*), \ldots$ are known observable parameters ϕ_k, that can be expressed in function of the model's parameter p. Consequently, with this approach the exhaustive summary is:

$$y^k(p,t^*) = \phi_k, \qquad k = 0,1,2,\ldots \tag{4.3}$$

where k is the derivative order. If it is possible to find an unique solution for p, the model is *a priori* identifiable. A drawback of this method is the impossibility to know how many derivatives (k) are needed for proving the unique identification of p. Moreover, due to the complexity that eq. 4.3 can reach, if no solution with respect to p is found, it does not mean that the model is not identifiable.

Other methods to solve the structural identifiability problem of non linear systems are present in literature, like the software *DAISY* (Differential Algebra for Identifiability of SYstems) [44], that exploits a **different algebra and geometry** approach.

4.1.2 Parameter estimation

After assessing the *a priori* identifiability, to assign a numerical value to the model's parameters, data collected from the system are needed. Since the parameter estimation is performed following the experiment, it is called *a posteriori* identification. Estimation of unknown parameters of mathematical models is not a trivial problem; in literature, many techniques exist and the approaches can be very different. However, all of them are estimators, statistics used to estimate an unknown true parameter $p \in \mathbb{R}^m$ exploiting the measured data $z \in \mathbb{R}^n$. An **estimator** ($\hat{p}(z)$) is a random variable, since measurements are random variables too, due to the additional random noise (the measurement error). A good estimator must have these properties:

- it is *unbiased*. Its expected value is equal to the true value of the unknown parameter: $E[\hat{p}] = p$;

- it is *consistent*. So if n grows, its mean square error $MSE(\hat{p})$ tends to zero: $\lim_{n\to\infty} E[(\hat{p} - E[\hat{p}])^2] = 0$. Since $MSE(\hat{p}) = Var(\hat{p}) + Bias(\hat{p})^2$, it means that the variance of $\hat{p}$ should tends to zero.

In mathematical notation, the output of the system in the scalar case is (discrete time domain):

$$y_k = g(t_k, p) \qquad k = 1, 2, ...n \tag{4.4}$$

where g in the function describing the model. If the model perfectly resembles the system, it should have the exact same behaviour of the system itself in all conditions. The formulation that connects measured data (z_k) and the model output can be written as follow:

$$z_k = y_k + v_k = g(t_k, p) + v_k, \qquad k = 1, 2, ...n \tag{4.5}$$

where v_k is the k-th sample of the measurement error corrupting z_k and it is an unknown random variable. Usually, some assumptions on the statistical distribution of v are proposed. It is generally considered normally distributed, with an expected value equal to zero and a known covariance matrix that can be factorized as $\Sigma_v = \sigma^2 B$. Samples of v are usually assumed uncorrelated, consequently B is usually a diagonal matrix.
For the following formulations is useful to put eq. 4.5 into a matrix-vector form, that contains all the measurements:

$$z = y + v = G(p) + v. \tag{4.6}$$

where $z, y, v \in \mathbb{R}^n, p \in \mathbb{R}^m$.

As this equation suggests, biological models are usually not linear in the parameters (it is not possible to write eq. 4.6 as $z = Gp + v$) that's why there isn't an analytical solution to find p and iterative methods have to be used. As a result, parameter estimation has an iterative nature (fig.4.2).

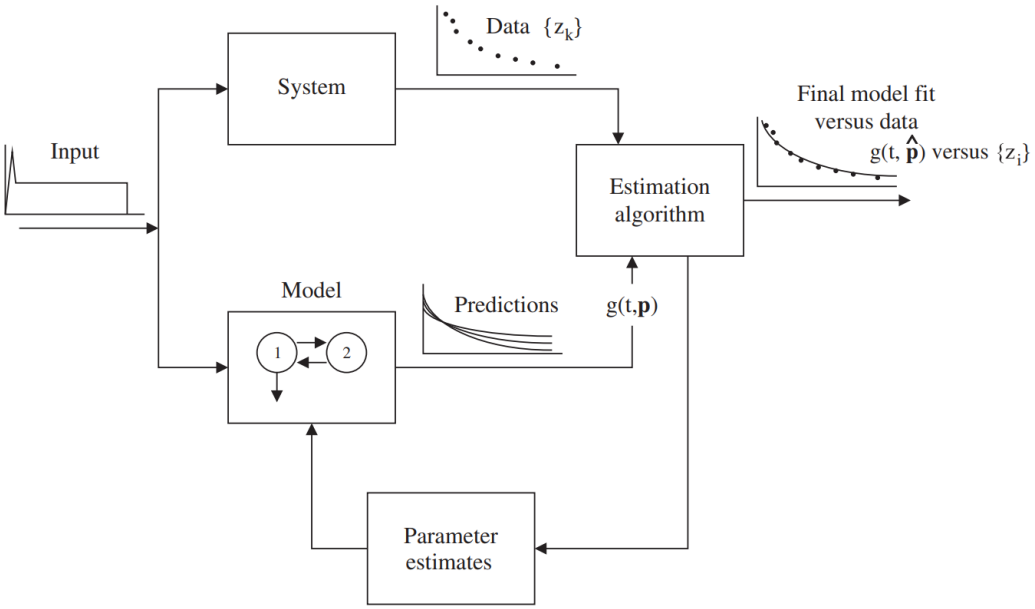

Figure 4.2: Iterative procedure for parameter estimation in case of model non linear in the parameters. Credit: Cobelli C., Carson E. [43].

Two main estimation approaches exist. A deterministic one (also called Fisher approach), for which it exits a true (unique) value of p, and it is estimated only using experimental data. A stochastic approach (also called Bayesian approach), where all involved variables are considered random values. Consequently, the output of the procedure is not only a point estimate of p, rather a statistical description in terms of its probability distribution function (pdf). In this case, not only measured data but also information prior to the experiment are exploited in the estimation process.

Deterministic approaches

A well known deterministic approach is based on weighted non linear least squares (WNLLS) estimation. Optimal p is the one that minimizes the quadratic distance between the data and the model prediction, i.e.:

$$\hat{p}^{WNLLS} = \arg\min_{p}[z - G(p)]^T \Sigma_v^{-1}[z - G(p)] \tag{4.7}$$

with $r = z - G(p)$ the residual vector, where each value is weighted with respect to its own uncertainty (inverse of the std of that sample). To find $\hat{p}^{WNLLS}$ the **Gauss-Newton Method** is used. It is an iterative procedure that works on the first order Taylor series approximation of the model. It calculates the gradient of the cost function with respect to the parameter vector and it updates the solution moving in the

direction opposite to the gradient. The update step is the one that minimizes the residual vector. One possible drawback of this procedure (and all similar gradient-based techniques) is the risk to stop the iterative procedure in a local minimum, instead of the desired global one, and consequently obtaining a wrong estimate of the unknown parameter vector. This approach provides also an estimation of the precision of the estimated parameters, in terms of the covariance matrix of the error vector $\tilde{p} = p - \hat{p}$, that is:

$$\Sigma_{\tilde{p}} \cong (S^T \Sigma_v^{-1} S)^{-1} \tag{4.8}$$

where S is the sensitivity matrix, that contains the gradient of $G(\hat{p})$ for each time point.

This is fundamental to calculate the coefficient of variation (CV) of the estimates, that is formalized as:

$$CV_{\hat{p}} = \frac{\sqrt{\sigma_{\tilde{p}}^2}}{\hat{p}} \tag{4.9}$$

where $\sigma_{\tilde{p}}^2$ is the variance of $\tilde{p}$ (the diagonal of $\Sigma_{\tilde{p}}$).

Another common approach to estimate p is the **maximum likelihood estimator (MLE)**. It exploits information regarding the probability density function of the measurement error $f_v(v)$ (if it is known or there is an assumption on it). Since v is an aleatory variable z is random too. As a result, it has its own pdf $f_z(z)$. Given eq. 4.6, pdf takes the following form:

$$f_z(z) = f_{G(p)+v}(G(p) + v) \tag{4.10}$$

When the experiment is realized, v is not a random variable anymore and it becomes one of its own realization v_{meas}, thus eq. 4.10 is a function of p only:

$$f_{G(p)}(G(p)) = L(p) \tag{4.11}$$

that is called *likelihood function of* p. The goal of the procedure is to find $\hat{p}$ that maximizes $L(p)$.

$$p^{\hat{MLE}} = \arg\max_p L(p) \tag{4.12}$$

In other words, MLE tries to fit a distribution on the experimental data and find the parameters of the distribution that better describes it. Also with this approach,

an estimation of the precision of the estimated parameters is provided. In fact, the Cramer-Rao inequality holds and it gives a lower bound to the estimated covariance matrix of $\tilde{p}$:

$$\Sigma_{\tilde{p}} \geq [F(p)|_{p=\hat{p}}]^{-1} \tag{4.13}$$

where $F(p)$ is the Fisher information matrix (FIM) that is the generalization of the *Fischer information (FI)* in the scalar case [45]. FI is a way to measure the amount of information that a random variable X carries about an unknown parameter θ of a distribution that models X. It is defined as the variance of the first derivative of the log-likelihood respect to θ (usually called score). Connecting this notation with the previous one, the random variable X is the vector of the measurements z and the unknown parameter θ is the vector containing the model parameters p. Therefore:

$$F(p) = E\left[\frac{\partial ln[L(p)]}{\partial p}\frac{\partial ln[L(p)]}{\partial p}^T\right] \tag{4.14}$$

In case of Gaussian and independent v, FIM is expressed as:

$$F(p)|_{p=\hat{p}} = S^T\Sigma_v^{-1}S \tag{4.15}$$

Stochastic approaches

The Bayesian stochastic approach is based on **Bayes's theorem**. To quickly understand it, let us see an example. A sample of 2600 people is divided based on sex (variable X) and height (variable Y), that is treated as a categorical variable with two classes: higher than 170 [cm] or lower. Division in the four groups (since there are two categorical variables each of them with two categories) is displayed in table 4.1.

		Height	
		<170 cm	>170 cm
Sex	M	500	1000
	F	700	400

Table 4.1: Sample of 2600 people divided according to their sex and height (simulated example).

From probability theory, for each cell of the table,the following general equation holds:

$$\begin{array}{c} p(X=x)p(Y=y|X=x) \\ = \\ p(Y=y)p(X=x|Y=y) \end{array} \qquad x=x_1,x_2; y=y_1,y_2. \tag{4.16}$$

where, for example, $p(Y = y|X = x)$ is the conditional probability of event y when event x is verified.
Thus, for instance:

$$\begin{array}{c} p(Height<170)p(sex=F|Height<170) \\ = \\ p(sex=F)p(Height<170|sex=F) \end{array} \tag{4.17}$$

Let us try to answer to the following question: "If a random person is selected from the group and his/her height is lower than 170 cm, is it possible to know if is female or male?".

It is impossible to be 100 % sure, however exploiting eq.4.16, it is possible to say that the person will be male or female with a certain probability:

$$p(sex = F|Height < 170) = \frac{p(Height < 170|sex = F)p(sex = F)}{p(Height < 170)} = 58.33\ \%$$
$$p(sex = M|Height < 170) = \frac{p(Height < 170|sex = M)p(sex = M)}{p(Height < 170)} = 41.66\ \% \tag{4.18}$$

Previous equations are exactly applications of Bayes's theorem. Let us think about measuring the height of each person of the group as the experiment performed in a study on this sample. Before the experiment, some ingredients of Bayes's theorem were already available. We are referring to $p(sex = F)$ and $p(sex = M)$. As a result, they are called *a priori probabilities* of the variable we want to predict (sex). After the experiment, we can measure how many person are smaller than 170 [cm] in both classes respect to sex ($p(Height < 170|sex = F)$ and $p(Height < 170|sex = M)$). This gives us a measure of how probable (likely) is to have a person smaller than the height threshold in both classes. This is the *likelihood function* or simply *likelihood* and it is a function of sex. Lastly, it is possible to calculate $p(Height < 170)$ simply as the sum of $p(Height < 170|sex = F)p(sex = F))$ and $p(Height < 170|sex = M)p(sex = M)$. All these ingredients made possible the calculation of $p(sex = F|Height < 170)$ and $p(sex = M|Height < 170)$ that are called *a posteriori probabilities*, since they are the probability of selecting a male or a female after the experiment (so after having measured some data).

This example can be generalized to m variables for which to calculate the a posteriori probability (it will be the model parameter vector that need to be estimated, p) and for n measured variables, also continuous variable and not just categorical (they will be the measured data of the experiment, z). Of course with continuous variables, to estimate the a posteriori probability $f_{p|z}(p|z)$, m-dimensional integral should be solved:

$$f_{p|z}(p|z) = \frac{f_{z|p}(z|p)f_p(p)}{\int_{\mathbb{R}^m} f_{z|p}(z|p)f_p(p)dp} \tag{4.19}$$

This is Bayes's theorem in the general case. $f_p(p)$ is the prior probability density function of p and $f_{z|p}(z|p)f_p(p)$ is the likelihood. Due to the need of solving high dimensional integrals, calculating the a posteriori pdf is not simple. Usually, there is the necessity of sampling methods (like Markov Chain Monte Carlo, MCMC) that are able to approximate $f_{p|z}(p|z)$ drawing samples from a distribution that tends to

it. Moreover, estimating the complete statistical description of p might be unpractical and one could be more interested in a point estimator of p from z. For instance, one could want to estimate p which maximizes the *a posteriori* distribution (*Maximum a posteriori*, MAP)

Luckily, in case of Gaussian distribution of p and v, this estimation problem can be solved as an optimization problem, since the optimal $p^{\hat{MAP}}$ can be found as:

$$p^{\hat{MAP}} = \arg\min_{p}[z - G(p)]^T \Sigma_v^{-1}[z - G(p)] + (p - \mu_p)^T \Sigma_p^{-1}(p - \mu_p) \tag{4.20}$$

This cost function is similar to the one of the WNLLS estimation (eq.4.7). However, here the second part of the function is taking into consideration the adherence of the estimated parameter vector to the a priori information (mean μ_p and covariance matrix Σ_p of $f_p(p)$).

Also with a Bayesian approach is it possible to get an estimation of the precision of the estimates. The formulation exploits the Cramer-Rao inequality (eq.4.13). For MAP estimation with Gaussian prior, Fisher information matrix takes the following form:

$$F(p)|_{p=\hat{p}} = S^T \Sigma_v^{-1} S + \Sigma_p^{-1} \tag{4.21}$$

As a result, precision of p will be better with this approach respect to deterministic ones. On the other hand, fit of the model to the data will be worse compared to WNLLS and MLE, since in the cost function of MAP a balance between fitting the data and matching prior information is realized.

The increased complexity of a stochastic approach respect to Fisher's ones is worth accepting in case of experiments with:

- low number of measured data (z);
- high uncertainty of z;
- estimation of complex model (high number of parameter to estimate).

A closing remark on the **algorithms** used to minimize the cost function defined by each approach, is worth doing. They can be divided into two categories: gradient-type algorithms and direct search algorithms. The first ones are based on the Gauss-Newton method, thus the calculation of the gradient is necessary. The second ones are faster methods since they avoid the calculation of any partial derivative. Therefore, they can span a wider range of possible solutions. The main drawback of these

methods is that they do not provide the precision of the estimated parameters. Consequently, gradient-type algorithms are the most used.

4.1.3 Identification strategy

As seen in the section related to the experimental design (sec.2.1), each subject was studied in two occasions, one with a suppressed glucose (S) infusion and one with a not suppressed infusion (NS). Ideally, if we identify the same model in the two occasions separately, even if inputs and measurements were different, we should estimate the same model parameters (figure 4.3).

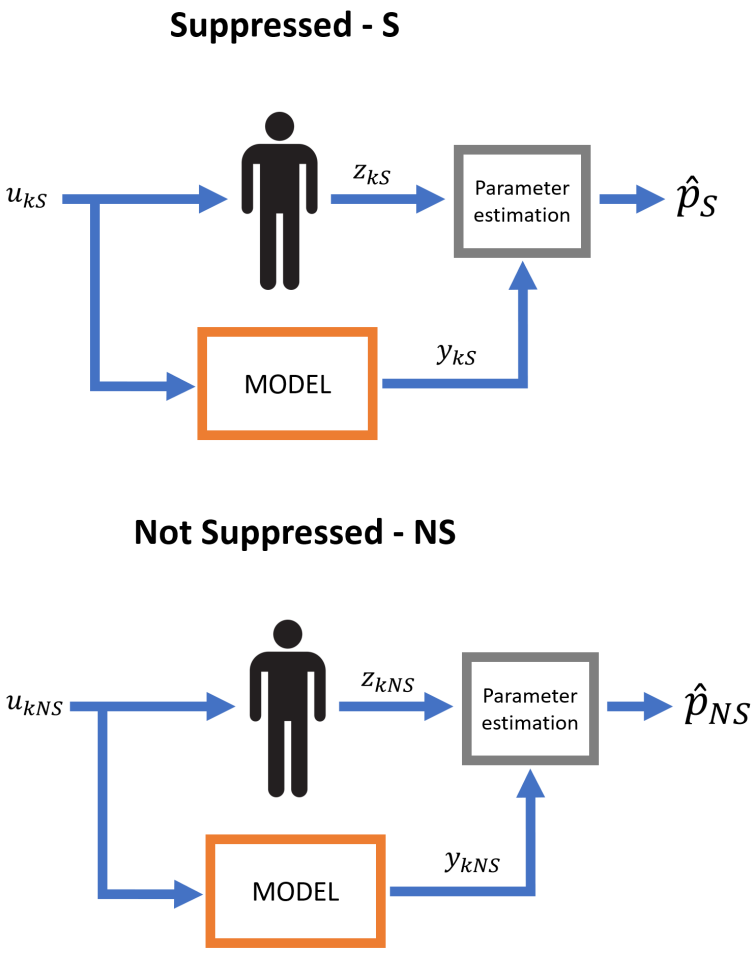

Figure 4.3: Parameter identification of a generic subject in the two experiments, S and NS. k is the k-th measurement.

Thus, $\hat{p}_S = \hat{p}_{NS}$. However, this is an ideal scenario since it assumes that the model is 100 % correct and *intra-subject variability* is absent. Unfortunately, the same subject undergoing the same experiment in two different occasions will respond to

the same input in different ways, due to some intrinsic unpredictable variability. In addition, the superimposed noise, like the measurement error, may have an impact in the accuracy of parameter estimates. Consequently, another estimation strategy should be used. A possible approach is a simultaneous identification that is to identify an unique parameter vector using data from both occasions. For example, with a deterministic approach like WNLLS (since all the proposed model structures of EGP are not linear in the parameters), $\hat{p}$ is the one that minimizes the following cost function:

$$J(p) = J_S(p) + J_{NS}(p) \tag{4.22}$$

Where $J_S(p)$ and $J_{NS}(p)$ are the cost functions of the two experiments defined as in eq. 4.7.
This approach produces an unique parameter estimate but the fit of the model in the two occasions could be likely not satisfactory. Since with this approach, intra-subject variability is not taken into account and the model is not "free" to adapt to data.

Thus, a better approach is to estimate two parameter vectors, one for each occasion, and put a constrain to force them to be close one to each other. In this way, intra-subject variability is taken into account, and the final estimates will be similar, but not equal, in the two experiments (the problem of separated identification is solved). The question is now how to define such a constrain. Before performing the experiment, *a priori*, we know that $\hat{p}_S$ and $\hat{p}_{NS}$ do not differ much. Thus, a Bayesian approach may be indicated. Furthermore, almost all of the proposed model structures of EGP have a large number of parameters that have to be estimated (18 in the most complex model). Since the number of available EGP data points, in case of simultaneously identification is at maximum 38, a deterministic approach provides estimates with a really high uncertainty. For the above reasons a MAP estimation approach was used. The proposed constrain is the following:

$$\hat{p}_{NS} = \hat{p}_S \circ \alpha \tag{4.23}$$

Where $\circ$ is the element-wise product and α is a vector with the following a priori information: $\alpha \sim N(\mu_\alpha; \Sigma_\alpha)$. μ_α is a vector of ones with the same dimensions of $\hat{p}_S$. With this formulation we are telling to the model that prior to the experiment the parameter vector in the two occasions is the same, and intra-subject variability is incorporated into Σ_α. With the Bayesian approach the cost function to minimize becomes:

$$J(p_S, \alpha) = J_S(p_S) + J_{NS}(p_{NS}) + [a - \mu_\alpha]^T \Sigma_\alpha^{-1} [a - \mu_\alpha] \tag{4.24}$$

Therefore, a compromise between fitting the data in the two experiments and having close estimates in S and NS is realized.

Identification of linear models of EGP

To identify model parameters of linear models of EGP, we used the identification strategy just described. Standard deviation of measurement error was assumed equal to 1 $[\mu mol/Kg/min]$. Estimation of parameters was done using *lsqnonlin* function of Matlab (R2020b). It uses an efficient algorithm based on the Gauss-Newton principle. Parameter initial values were fixed according to previous models present in literature ([25],[39]).

Identification of non linear models of EGP

Unlike linear models, non linear ones were not based on a previous model proposed in the literature. To better test model structure ability to fit the data, we decided to set less possible constrains in the initial identification approach. That's why, we identified separately the model on S and NS occasion, using a deterministic approach. In fact, if the fitting result was not acceptable with separate identification, with a simultaneous one the fit would have been even worse. Using the Fisherian approach provided the possibility of not assuming the standard deviation of the measurement error of EGP, and to estimate it a posteriori (instead with a Bayesian approach, this was not possible). Furthermore, we used the Matlab (R2020b) function *fminsearch* that is based on a direct search algorithm. Since we did not have information about plausible initial values of the parameters, we preferred to use this type of algorithm instead of a gradient-type one, to explore a wider range of possible solutions.

4.1.4 Model assessment

After the parameter estimation stage, an assessment of the identified model must be performed. This step focuses mainly on fitting performances and precision and plausibility of the estimated parameters.

Goodness of fit

If the model is correct, in the sense that it is able to perfectly reproduce the system behaviour in the experimental setting, from eq.4.6 it is easy to retrieve that the residuals of the model should be equal to the additive measurement noise:

$$r = z - G(\hat{p}) = v \tag{4.25}$$

Consequently, since v was assumed as a white noise with a known variance, r should have the same statistical properties. Firstly, residual should be uncorrelated and secondly their amplitude should be the same of the measurement error. An usual approach is to display weighted residuals, $wres$, that are residual weighted with the standard deviation of v. The variance of the k-th $wres$ is:

$$var(wres_k) = var(\frac{r_k}{\sigma_k}) = \frac{1}{\sigma_k^2} \cdot var(r_k) = \frac{1}{\sigma_k^2} \cdot var(v_k) = 1 \tag{4.26}$$

For this reason, on average the 66 % of $wres$ should lay inside the [-1,+1] band. To evaluate amplitude and whiteness, an initial visual inspection is performed. Then, a more robust approach to assess whiteness is applying an Anderson-Darling test [46]. A quick metric to evaluate fitting performance of the model is to calculate the *wighted residual sum of square (WRSS)*, as follow:

$$WRSS = r^T \Sigma_v^{-1} r \tag{4.27}$$

The lowest WRSS is and the better the model is able to fit the data.

Precision and plausibility of the estimated parameters

Both Fisherian and Bayesian techniques supply an estimation of the uncertainty of the estimates (eq. 4.15 and eq. 4.21). This uncertainty is usually expressed by the coefficient of variation of the estimates (eq. 4.9). Estimated parameters will have a good precision if their CV is under 50 %. A CV slightly higher can be accepted for few parameters, in particular in case of complex model structure. If CV is greater then 100 %, there is a too high uncertainty on the estimation of that parameter. Another fundamental aspect to take into consideration is the plausibility of parameter values. Thus, if there is a physiological foundation that confirms the credibility of the estimated values. For some parameters, this can be obvious (for example a transfer rate coefficient [1/min] cannot be negative), for others it might be difficult to find

information in the literature (for example if you are building a novel model for which there are not well known benchmarks).

4.1.5 Model selection

After the model assessment step, if all metrics are satisfied, the modelling process has produced a reasonable model of the analyzed system, at least in the defined **domain of validity**. Since several model structures can successfully pass through the whole procedure is important to have a defined and robust methodology to compare models and select the best one. Particular useful are the so called **parsimony criteria**. They are statistical metrics that evaluate how good is a model (in term of fitting performance) with respect to its complexity (number of model parameters). In fact, it is well known that more complex models are better able to fit the data, since they have more degrees of freedom. As a drawback, such complex models may adapt to much to the experimental data and suffer from the *overfitting problem*. Therefore, parsimony criteria realize a balance between fitting and model complexity, that reflects a balance between bias and variance of the model. For Bayes estimation a common parsimony criterion is the Generalized Information Criterion (GEN-IC) [47], defined as:

$$GEN - IC = \frac{2m}{n} + J(\hat{p}) \tag{4.28}$$

where, as seen before, m is the number of parameters of the model, n is the number of available data points and $J(\hat{p})$ is the cost function defined as in eq.4.24, evaluated in $\hat{p}$. Another two popular criteria are the Akaike Information Criterion - AIC (eq. 4.29) and the Bayes Information Criterion - BIC (eq. 4.30). Both of them are based on the same principle of balancing between goodness of fit and model complexity. BIC has an higher penalty for model complexity respect to AIC (if n > 7).

$$AIC = WRSS + 2m \tag{4.29}$$

$$BIC = WRSS + mlog(n) \tag{4.30}$$

In case of small sample size , a correct version of AIC is used (eq. 4.31).

$$AICc = AIC + \frac{2m(m+1)}{n-m-1} \tag{4.31}$$

The best model is that one with the lowest value of parsimony criteria.

4.1.6 Statistical analysis

As seen in the experimental design section 2.1, this study tried to mimic the impaired glucagon suppression (IGS) of T2DM patients after a meal challenge (not suppressed occasion), and also how different defective insulin secretions (0.6/0.8 Ins. group), with respect to normal (1.0 Ins. group), can impact glucagon action on hepatic glucose production. Therefore, it is interesting to see how parameters of the selected model change according to insulin secretion level and glucagon profile. They can be thought as the two factors that may influence model parameters. That is why, *two-way analysis of variance (ANOVA)* is the optimal tool to evaluate results from a statistical prospective, taking into consideration the influence of both factors. ANOVA evaluates if samples from 2 or more groups came from the same statistical distribution, calculating intra and inter group variances. The null hypothesis is that all groups have the same sample mean, the alternative hypothesis is that at least one group has sample mean that differs from another group. ANOVA assumes that all groups are normally distributed and have the same variance (homoschedasticity). Even if the normality assumption is not properly satisfied, the test is robust enough to deal with it. However, if group variances are not equal, the results of ANOVA are weaker. For this reason, an homoschedasticity test is usually applied before ANOVA, for example the *Levene's test*. If ANOVA suggests to reject the null hypothesis (p-value lower than the selected level of significance α), it is not possible to know which group or groups have different mean with respect to the others. To understand it a *post hoc analysis* is performed. The simplest approach is to apply a *t-test* to all group couples. However, the main issue of multiple comparison procedures is that the probability of rejecting a null hypothesis when it is true (type 1 error) is not more equal to the chosen α. Consequently, we should focus on the overall probability of committing type 1 error, the so called family-wise error rate (FWER). To do so, several approaches are available in the literature, like the Bonferroni correction, the Sidak procedure and the Tukey's test. In particular, the last one is essentially a t-test corrected for FWER. Statistical analysis was performed in Matlab (R2020b).

5 Results

5.1 A priori identifiability

Model 1 and Model 2 are time-invariant and have a linear dynamics. Consequently, we used the transfer function method to test the *a priori* identifiability. Both models resulted to be globally identifiable. We obtained the same result using the software *DAISY*. Models 3, 4, 5, 6, 7 and 8 are still linear in the dynamics, however, they are not time-invariant due to the introduction of the glucagon evanescent effect $E(t)$ in the model structure. Exploiting the Taylor series expansion method, we proved that all models are *a priori* globally identifiable. *A priori* identifiability of non linear models was tested with the software *DAISY*. Non linear model 2, 3 and 4 resulted to be *a priori* globally identifiable. We were not able to prove the *a priori* identifiability of non linear model 1. However, as seen in section 4.1.1, it does not mean that the model is *a priori* not identifiable.

5.2 A posteriori identification

Model implementation and parameter identification was realized in Matlab (R2020b). Numerical integration of differential equations was performed using *ode45* solver implemented in Matlab (R2020b). Firstly, model identification and selection was based on model performance on average profiles. Since the "average subject" has the less noisy measurement data and input signals, due to the noise attenuation property of the averaging operation. Consequently, poor fitting performances on mean val-

ues will lead to even worst results at individual level. Then, the selected model was tested on individual subjects.

5.2.1 Linear models of EGP

Model 1

Model 1 (eq. 3.1) do not consider a glucagon contribution to model EGP profile. Since, this experiment was design to emphasise glucagon action on EGP, we expected poor fitting performance. This was confirmed by the identification results (fig. 5.1). In the S occasion the model was able to follow the EGP decrease in the first part of the experiment, since it was produced mainly by insulin infusion (that is taken into consideration by the model). The following EGP rise is due to the reduction of insulin infusion and increasing of glucagon concentration caused by its infusion at t = 120 [min]. The model was not properly able to follow this upswing, since it does not consider the glucagon action. In the NS occasion, the fit is better since glucagon is constantly infused during all the experiment. Thus, its effect on EGP is constant (if evanescence phenomenon is not considered). However, the fit is still not satisfactorily.
A remark about insulin and its action is worth doing: in both occasions concentration profiles are rather close. As a result, also similar insulin actions are expected. Even taking into account the intra-subject variability, such difference in insulin actions between the two experiments is not acceptable. Lastly, glucose derivative profile was not needed to fitting the data, that's why its action on EGP is almost null. Consequently, precision of the parameter related to glucose derivative action kp_7 is poor (CV»100%, see table 5.1). To wrap up, as predicted, this model did not provide acceptable results.

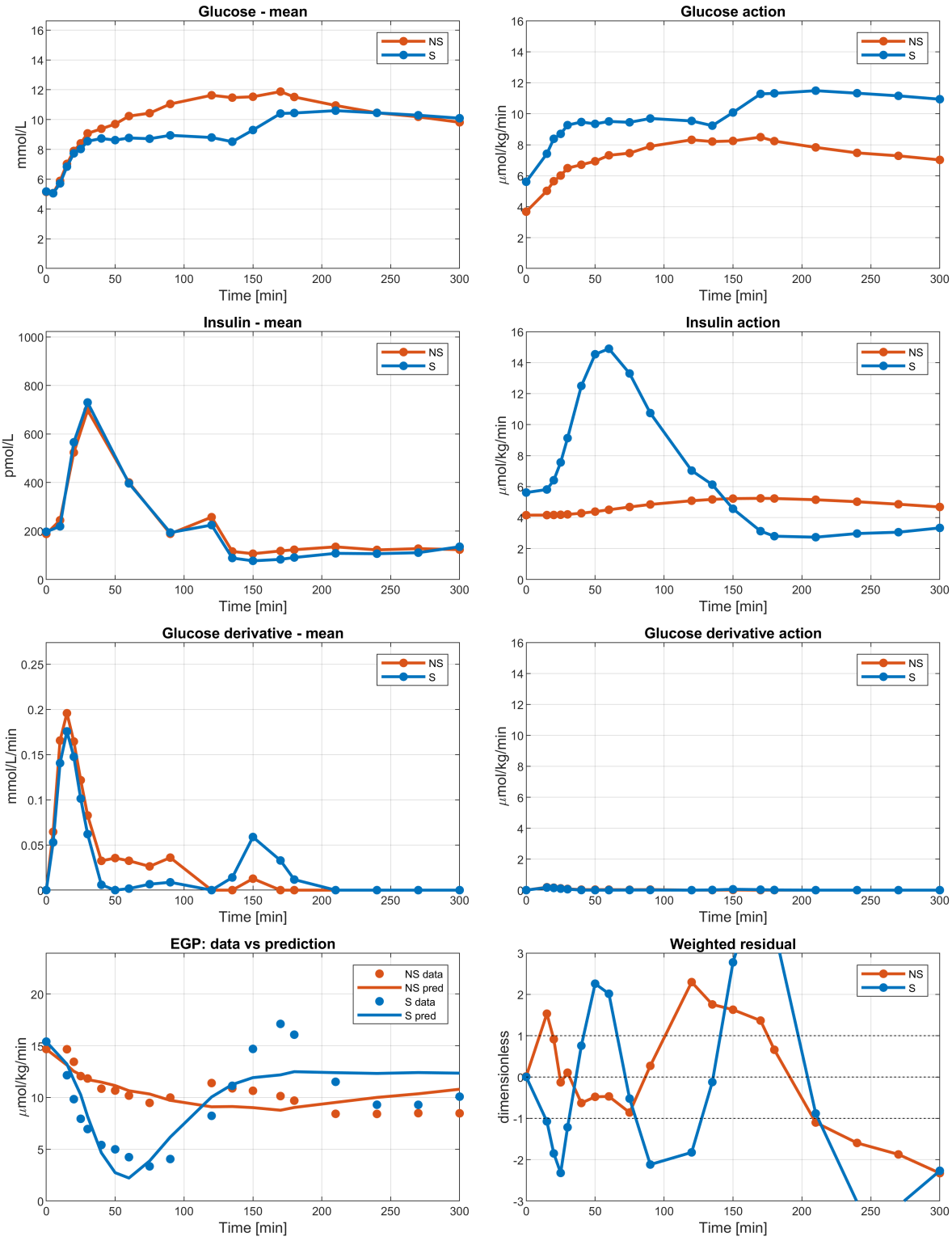

Figure 5.1: Model 1 prediction vs average EGP data: Rows 1-3: input signals (left panel) and relative actions on EGP (right panel); row 4: EGP data vs. model predictions (left panel) and weighted residuals (right panel) in both not suppressed (NS) and suppressed (S) occasions.

	NS		S	
Parameters	**value**	**CV(%)**	**value**	**CV(%)**
kp2 $\left[\frac{ml}{kg \cdot min}\right]$	0.713	14.1	1.080	5.7
kp3 $\left[\frac{\frac{\mu mol}{kg \cdot min}}{\frac{pmol}{l}}\right]$	0.023	25.8	0.030	5.4
kp5 $\left[\frac{1}{min}\right]$	0.006	55.5	0.070	1.8
kp7 $\left[\frac{ml}{kg}\right]$	0.970	289.0	0.960	288.4

Table 5.1: Results of Model 1 identified on average data: estimated parameters and their precision (CV) in both not suppressed (NS) and suppressed (S) occasions.

Model 2

Model 2 (eq. 3.2), takes into account glucagon concentrations to predict EGP, consequently better performances with respect to model 1 were a priori expected. Instead, as displayed in figure 5.2, model fit was comparable with that obtained with Model 1. Let us try to understand why. Firstly, the model was actually using glucagon profile to predict EGP, since glucagon action was present in both occasions (left panel of row 3). Especially in S case, glucagon could help the model to describe EGP rise after the first decrease. However, from $t \cong 170\ [min]$ EGP starts to decline again. This fall could not be explained with glucagon profile, since it remains constant after $t \cong 170\ [min]$. Therefore, a better fit of the EGP upswing (based on glucagon increase) produced a worst fit of the following EGP data points. With respect to Model 1, insulin actions estimated in the two occasions are closer, however, the inter-day difference was still too large to be acceptable.

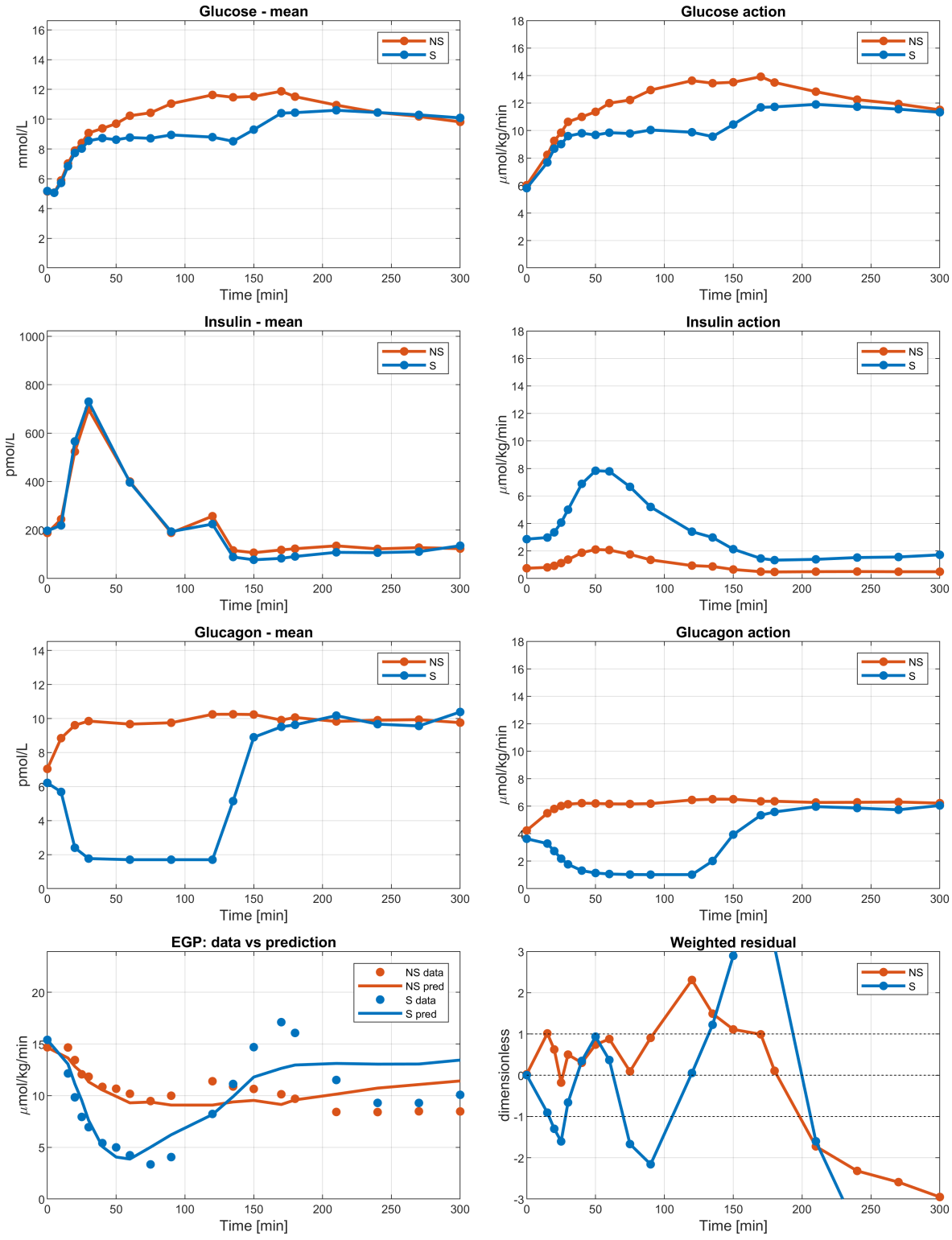

Figure 5.2: Model 2 prediction vs average EGP data: Rows 1-3: input signals (left panel) and relative actions on EGP (right panel); row 4: EGP data vs. model predictions (left panel) and weighted residuals (right panel) in both not suppressed (NS) and suppressed (S) occasions.

	NS		S	
Parameters	**value**	**CV(%)**	**value**	**CV(%)**
kp2 $\left[\frac{ml}{kg \cdot min}\right]$	1.165	11.0	1.120	5.7
kp3 $\left[\frac{\frac{\mu mol}{kg \cdot min}}{\frac{pmol}{l}}\right]$	0.003	46.4	0.010	19.2
kp4 $\left[\frac{\frac{\mu mol}{kg \cdot min}}{\frac{pmol}{l}}\right]$	0.636	28.3	0.600	22.0
kp5 $\left[\frac{1}{min}\right]$	0.087	17.0	0.080	0.2
kp6 $\left[\frac{1}{min}\right]$	0.187	0.0	0.100	0.0

Table 5.2: Results of Model 2 identified on average data: estimated parameters and their precision (CV) in both not suppressed (NS) and suppressed (S) occasions.

MODEL 3

Model 3 (eq.3.3) takes into consideration the glucagon evanescent effect. Its introduction solves the problem pointed out in model 2. In fact, glucagon action can be considered responsible of the rise and the following fall of EGP from $t \cong 120\ [min]$ in S occasion. Therefore, the fit of this model to the data was substantially increased with respect to the previous ones, in both occasions. Furthermore, the difference in insulin actions in S vs NS could be addressed to intra-subject variability. From a visual inspection of weighted residual, it can be seen that this model is still not properly resembling system behaviour. In particular, from $t = 0\ [min]$ to $t = 40\ [min]$ there was a negative peak in both cases. Thus, the model was not able to follow EGP downswing. Moreover, EGP rise in S was still underestimated. Precision of estimates was good for all parameters (table 5.3).

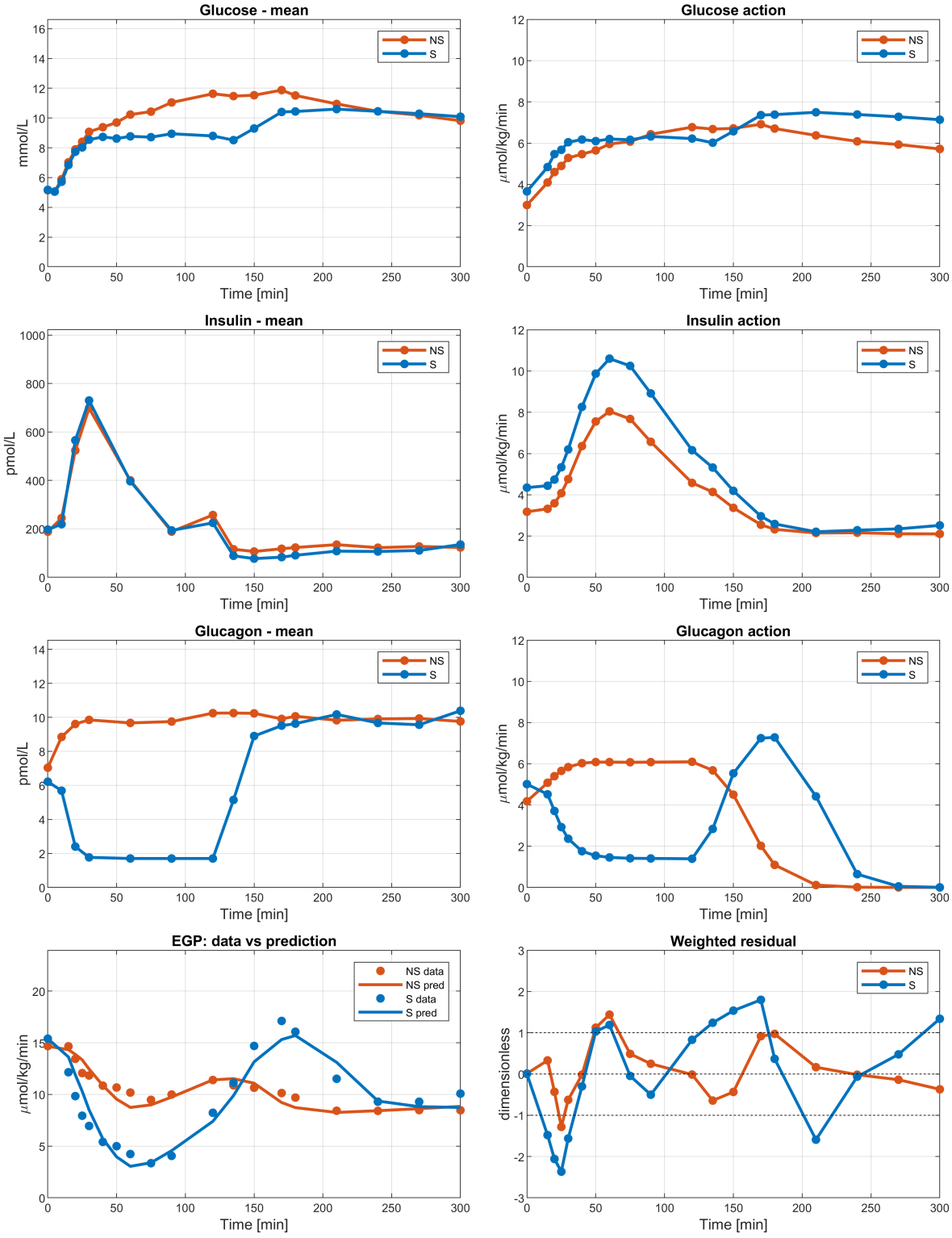

Figure 5.3: Model 3 prediction vs average EGP data: Rows 1-3: input signals (left panel) and relative actions on EGP (right panel); row 4: EGP data vs. model predictions (left panel) and weighted residuals (right panel) in both not suppressed (NS) and suppressed (S) occasions.

	NS		S	
Parameters	**value**	**CV(%)**	**value**	**CV(%)**
kp2 $\left[\frac{ml}{kg \cdot min}\right]$	0.582	19.6	0.710	13.3
kp3 $\left[\frac{\frac{\mu mol}{kg \cdot min}}{\frac{pmol}{l}}\right]$	0.015	20.5	0.020	8.9
kp4 $\left[\frac{\frac{\mu mol}{kg \cdot min}}{\frac{pmol}{l}}\right]$	0.631	21.3	0.830	14.4
kp5 $\left[\frac{1}{min}\right]$	0.055	17.8	0.050	10.9
kp6 $\left[\frac{1}{min}\right]$	0.096	22.1	0.110	0.8
$1/\tau$ $\left[\frac{1}{min}\right]$	0.037	46.9	0.040	42.1
t_0 $[min]$	160.370	11.7	91.640	8.4

Table 5.3: Results of Model 3 identified on average data: estimated parameters and their precision (CV) in both not suppressed (NS) and suppressed (S) occasions.

Model 4

In model 4 (eq. 3.4), glucagon was assumed to act without any delay and proportionally to glucagon concentration. With respect to Model 3, glucagon action was obviously less smooth. This gives to the model the ability to promptly follow EGP rise and fall (fig.5.4). The amplitude of weighted residuals was almost in the $[-1, +1]$ band. Regarding residual whiteness, uncorrelated residual are not expected due to the estimation process of EGP (more details in chapter 2, section 2.3). Consequently, from a visual inspection, they are satisfactory unless for a small negative peak in the initial part for both S and NS. Precision of the estimated parameter was good (CV < 50% for every parameter, tab. 5.4). To sum up, removing glucagon delay and using a component proportional to its plasma concentration improved model performances.

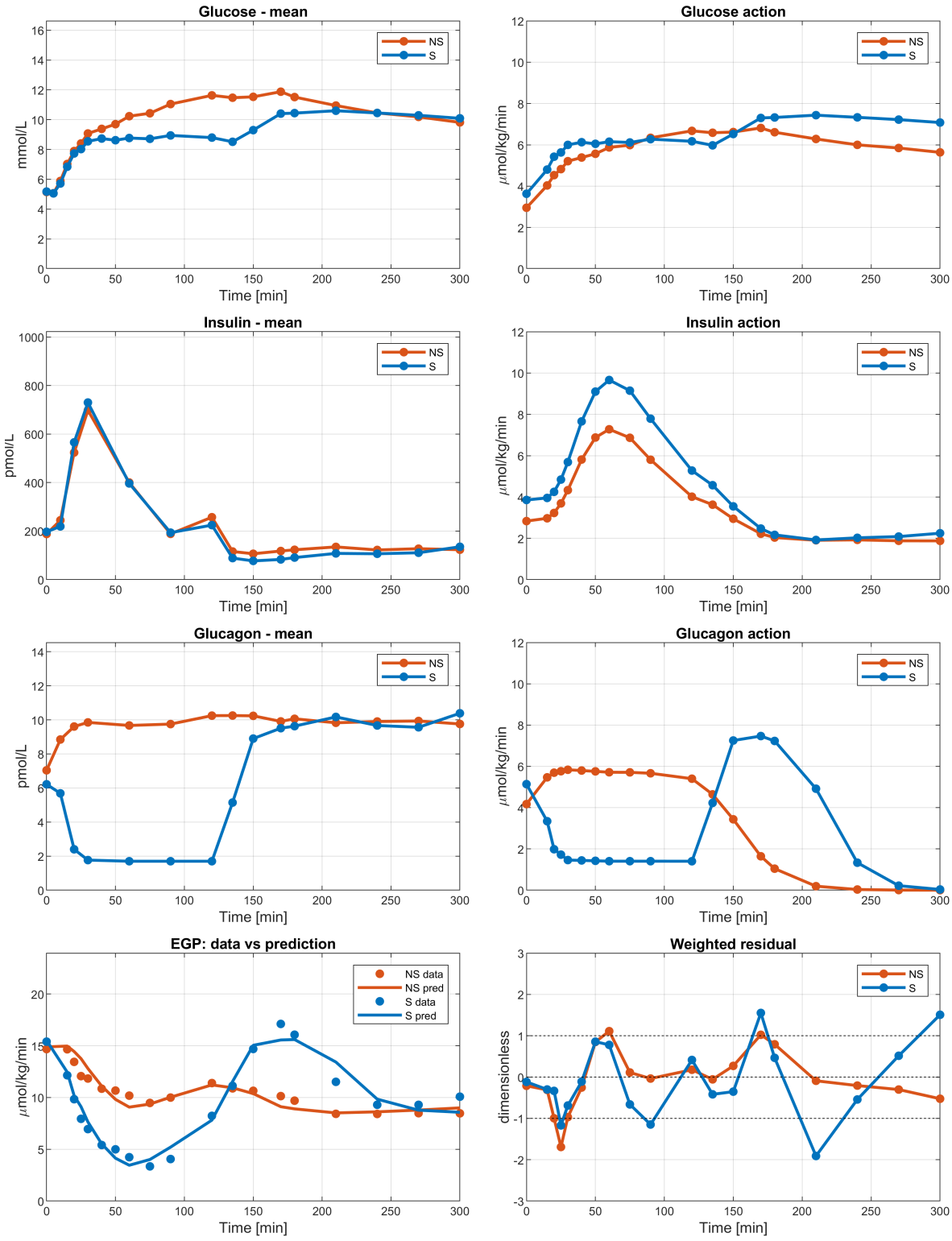

Figure 5.4: Model 4 prediction vs average EGP data: Rows 1-3: input signals (left panel) and relative actions on EGP (right panel); row 4: EGP data vs. model predictions (left panel) and weighted residuals (right panel) in both not suppressed (NS) and suppressed (S) occasions.

	NS		S	
Parameters	**value**	**CV(%)**	**value**	**CV(%)**
kp2 $\left[\frac{ml}{kg \cdot min}\right]$	0.574	20.7	0.702	14.5
kp3 $\left[\frac{\frac{\mu mol}{kg \cdot min}}{\frac{pmol}{l}}\right]$	0.015	22.6	0.020	13.1
kp4 $\left[\frac{\frac{\mu mol}{kg \cdot min}}{\frac{pmol}{l}}\right]$	0.593	20.5	0.827	12.7
kp5 $\left[\frac{1}{min}\right]$	0.062	15.9	0.059	6.7
$1/\tau$ $\left[\frac{1}{min}\right]$	0.030	41.7	0.033	36.4
t_0 $[min]$	154.390	12.5	95.261	9.0

Table 5.4: Results of Model 4 identified on average data: estimated parameters and their precision (CV) in both not suppressed (NS) and suppressed (S) occasions.

Model 5

Model 5 (eq. 3.5) is based on model 3 (eq. 3.3) with the addition of a component proportional to glucose rate of change, if it is positive. In row 4 of fig. 5.5, it can be appreciated that the main contribution of this new component is in the first 50 minutes of the experiment. Since glucose concentration in both occasions increases with an higher rate when the glucose infusion that mimic a prandial input started. Since glucose reduces EGP, also its rate of change has an inhibition effect. This helped to better follow the initial downswing of EGP respect to all previous models and it can be seen from the weighted residual graph (row 5, right panel). Mean CV of estimated parameters increases respect to model 3 (since a new parameter is estimated), however the precision is still reasonable.

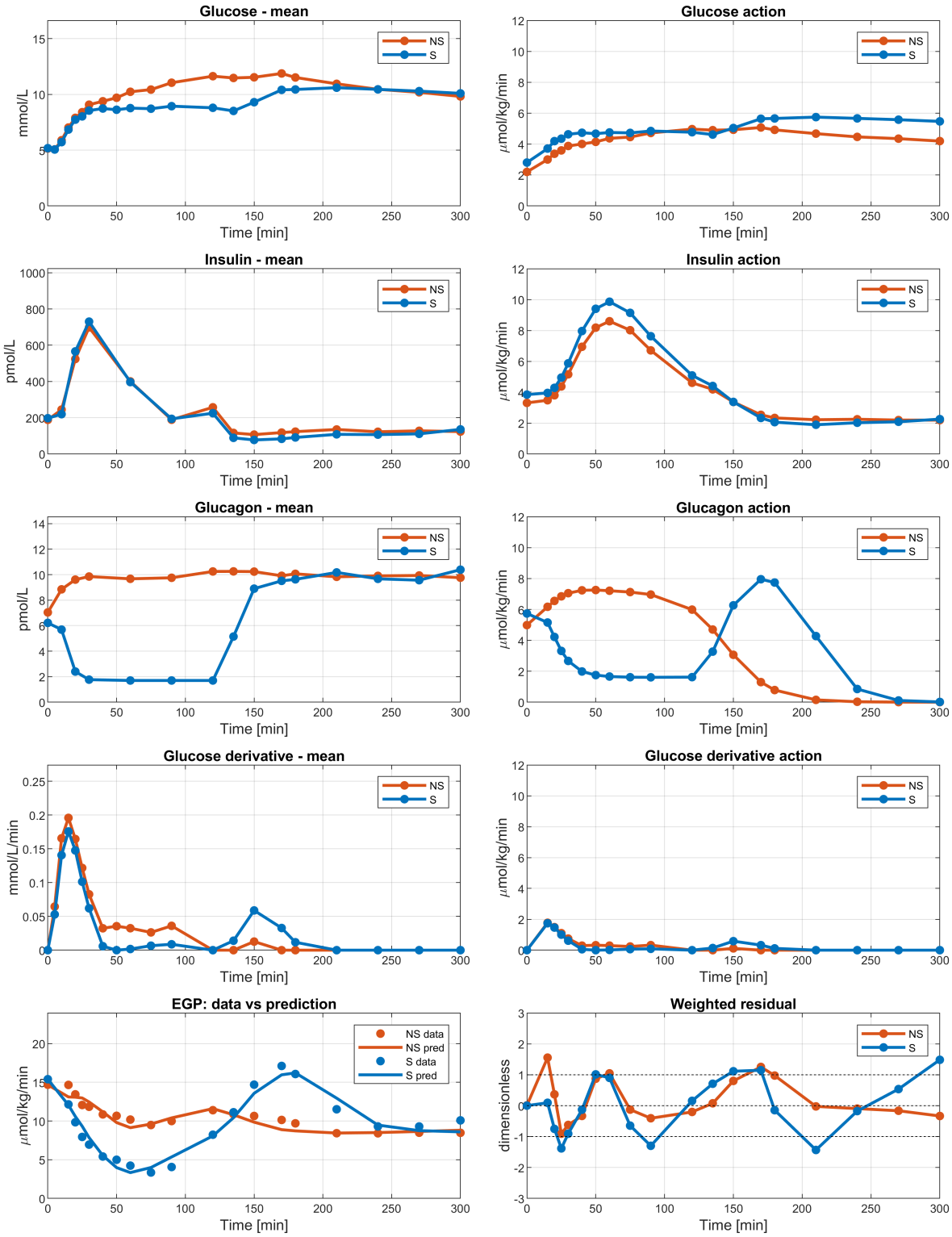

Figure 5.5: Model 5 prediction vs average EGP data: Rows 1-4: input signals (left panel) and relative actions on EGP (right panel); row 5: EGP data vs. model predictions (left panel) and weighted residuals (right panel) in both not suppressed (NS) and suppressed (S) occasions.

	NS		S	
Parameters	**value**	**CV(%)**	**value**	**CV(%)**
kp2 $\left[\frac{ml}{kg \cdot min}\right]$	0.427	32.2	0.540	26.1
kp3 $\left[\frac{\frac{\mu mol}{kg \cdot min}}{\frac{pmol}{l}}\right]$	0.018	21.8	0.020	12.9
kp4 $\left[\frac{\frac{\mu mol}{kg \cdot min}}{\frac{pmol}{l}}\right]$	0.751	23.4	0.950	16.1
kp5 $\left[\frac{1}{min}\right]$	0.061	14.4	0.060	0.8
kp6 $\left[\frac{1}{min}\right]$	0.110	28.2	0.110	20.2
$1/\tau$ $\left[\frac{1}{min}\right]$	0.025	42.4	0.030	36.0
t_0 $[min]$	143.123	11.7	87.270	8.8
kp7 $\left[\frac{ml}{kg}\right]$	9.027	43.1	9.920	37.7

Table 5.5: Results of Model 5 identified on average data: estimated parameters and their precision (CV) in both not suppressed (NS) and suppressed (S) occasions.

Model 6

As done with model 4 respect to model 3, model 6 (eq. 3.6) is equal to model 5 unless for a direct contribution of plasma glucagon in the stimulation of EGP. Signal actions on hepatic production were similar to the ones of the previous model, except for a less smooth glucagon action. Goodness of fit improved, leading to satisfactory results (fig. 5.6). Parameters' precision was good apart for k_{p7} with a CV slightly grater than 50%.

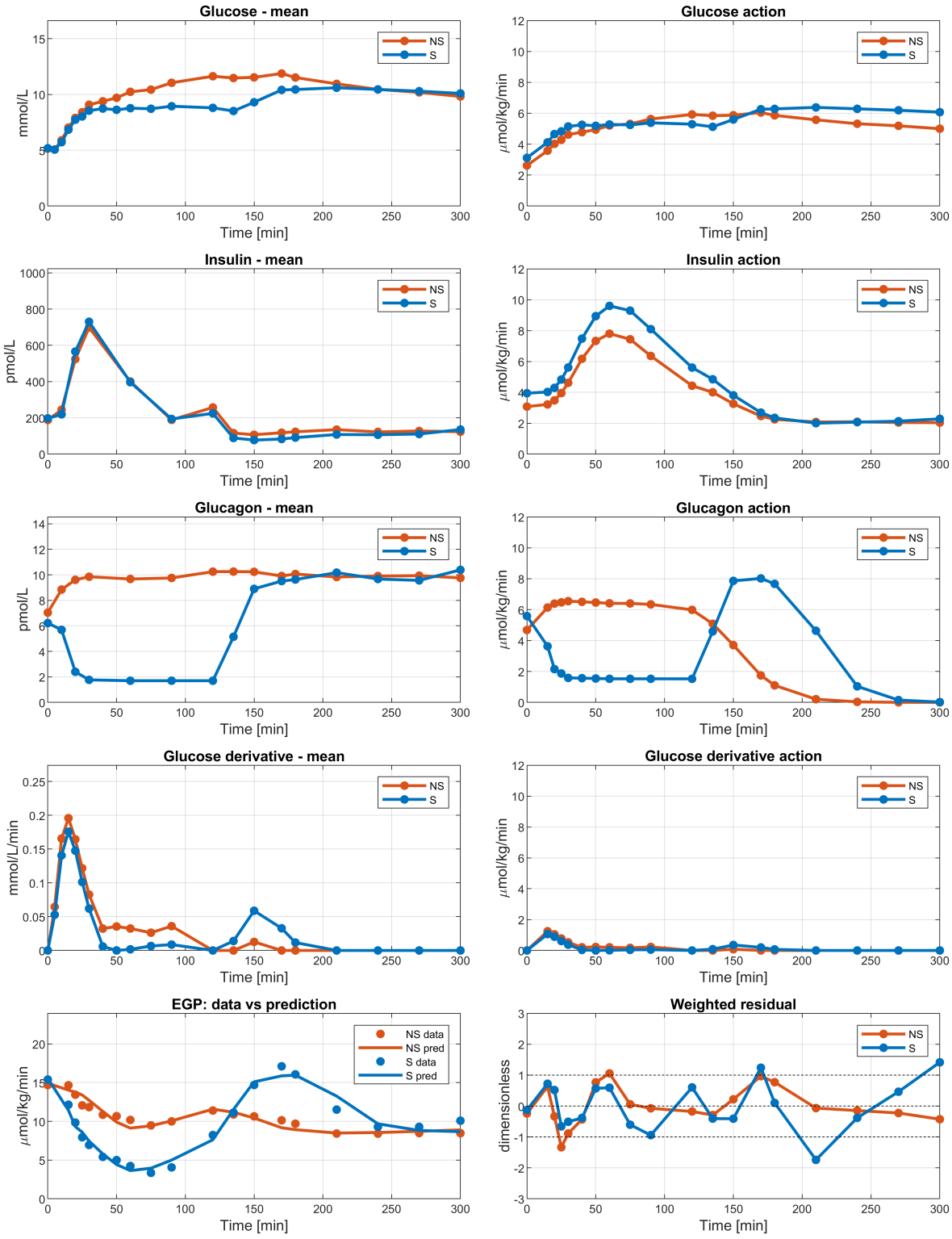

Figure 5.6: Model 6 prediction vs average EGP data: Rows 1-4: input signals (left panel) and relative actions on EGP (right panel); row 5: EGP data vs. model predictions (left panel) and weighted residuals (right panel) in both not suppressed (NS) and suppressed (S) occasions.

	NS		S	
Parameters	**value**	**CV(%)**	**value**	**CV(%)**
kp2 $\left[\frac{ml}{kg \cdot min}\right]$	0.509	24.2	0.602	18.0
kp3 $\left[\frac{\frac{\mu mol}{kg \cdot min}}{\frac{pmol}{l}}\right]$	0.016	20.5	0.020	10.1
kp4 $\left[\frac{\frac{\mu mol}{kg \cdot min}}{\frac{pmol}{l}}\right]$	0.665	19.3	0.898	12.0
kp5 $\left[\frac{1}{min}\right]$	0.060	18.0	0.054	10.3
$1/\tau$ $\left[\frac{1}{min}\right]$	0.030	40.9	0.034	34.9
t_0 $[min]$	152.937	11.0	90.442	8.0
kp7 $\left[\frac{ml}{kg}\right]$	6.364	55.2	6.033	52.0

Table 5.6: Results of Model 7 identified on average data: estimated parameters and their precision (CV) in both not suppressed (NS) and suppressed (S) occasions.

Model 7

Model 7 (eq. 3.7) is equal to model 3, plus a component proportional to glucagon rate of change, if it is positive. This new factor should help the model to better follow fast EGP increase, especially in the S occasion. As you can see from the left bottom panel of figure 5.7, this was true only for the first part of the upswing of EGP. Moreover, the fit was worst in the initial part of the experiment in both S and NS occasions. Consequently, the introduction of glucagon rate of change did not substantially help in these experimental settings.

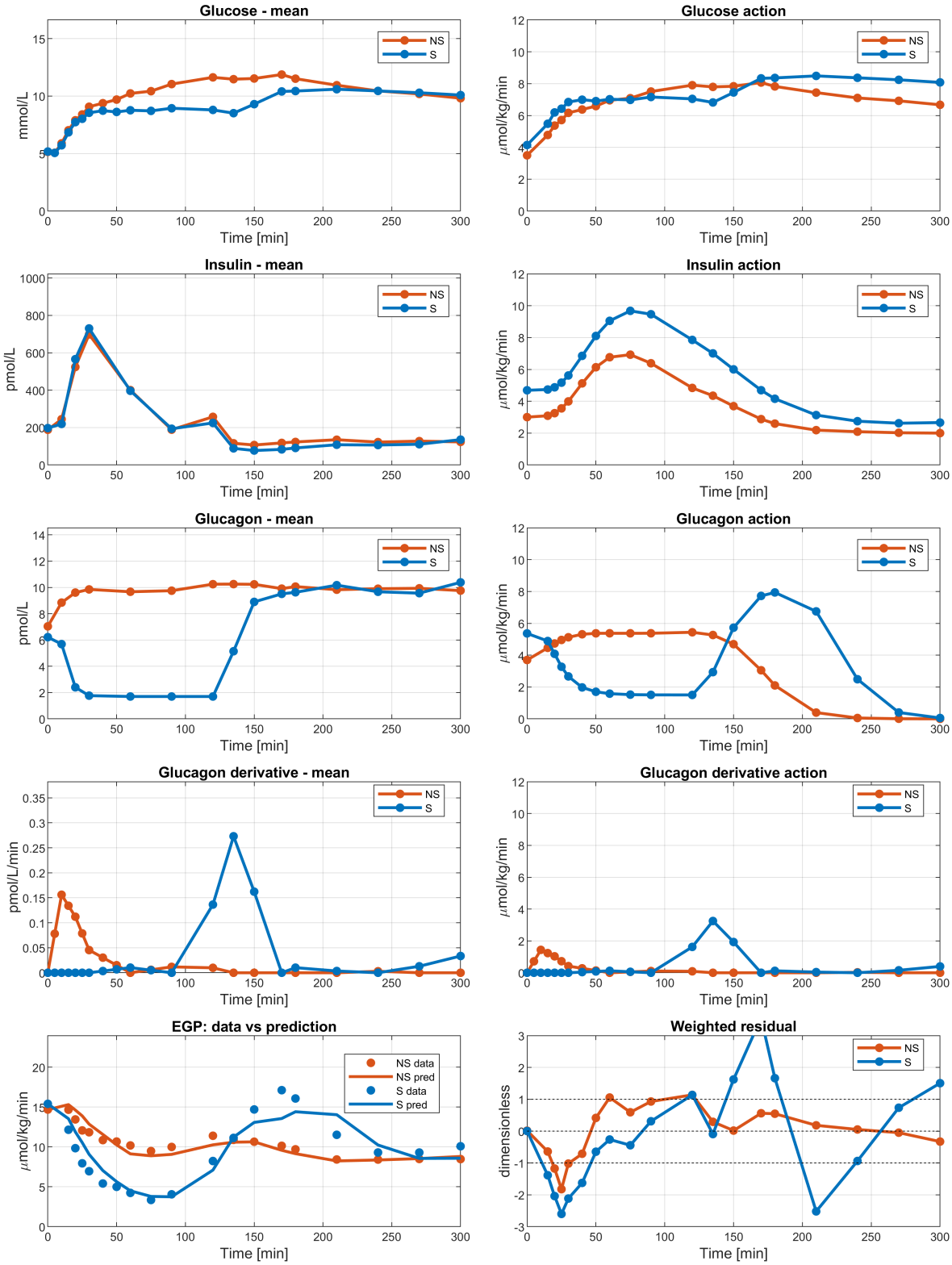

Figure 5.7: Model 7 prediction vs average EGP data: Rows 1-4: input signals (left panel) and relative actions on EGP (right panel); row 5: EGP data vs. model predictions (left panel) and weighted residuals (right panel) in both not suppressed (NS) and suppressed (S) occasions.

	NS		S	
Parameters	**value**	**CV(%)**	**value**	**CV(%)**
kp2 $\left[\frac{ml}{kg \cdot min}\right]$	0.680	18.9	0.800	13.1
kp3 $\left[\frac{\frac{\mu mol}{kg \cdot min}}{\frac{pmol}{l}}\right]$	0.013	26.8	0.020	15.1
kp4 $\left[\frac{\frac{\mu mol}{kg \cdot min}}{\frac{pmol}{l}}\right]$	0.554	23.7	0.880	14.8
kp5 $\left[\frac{1}{min}\right]$	0.040	20.8	0.030	15.9
kp6 $\left[\frac{1}{min}\right]$	0.090	22.1	0.100	0.0
$1/\tau$ $\left[\frac{1}{min}\right]$	0.029	56.6	0.030	53.0
t_0 $[min]$	172.190	13.4	106.950	9.8
kp8 $\left[\frac{\frac{\mu mol}{kg}}{\frac{pmol}{l}}\right]$	9.163	38.6	11.900	29.7

Table 5.7: Results of Model 7 identified on average data: estimated parameters and their precision (CV) in both not suppressed (NS) and suppressed (S) occasions.

MODEL 8

Model 8 is the most complex linear model tested and it includes all the different parts of previous models. Regarding insulin profiles and insulin actions in both occasions, it provided the best results: same insulin profiles lead to exactly same actions on EGP (fig. 5.8). Model prediction was good; as a result, weighted residual were good too. Probably, glucagon rate of change reduced the ability of the model to follow the first fall of EGP in NS (in particular around $t = 20 - 40$ $[min]$). On the other hand, It increased fitting performance in the EGP rise in S occasion. Despite the high number of parameters, estimation's precision was acceptable (tab. 5.8).

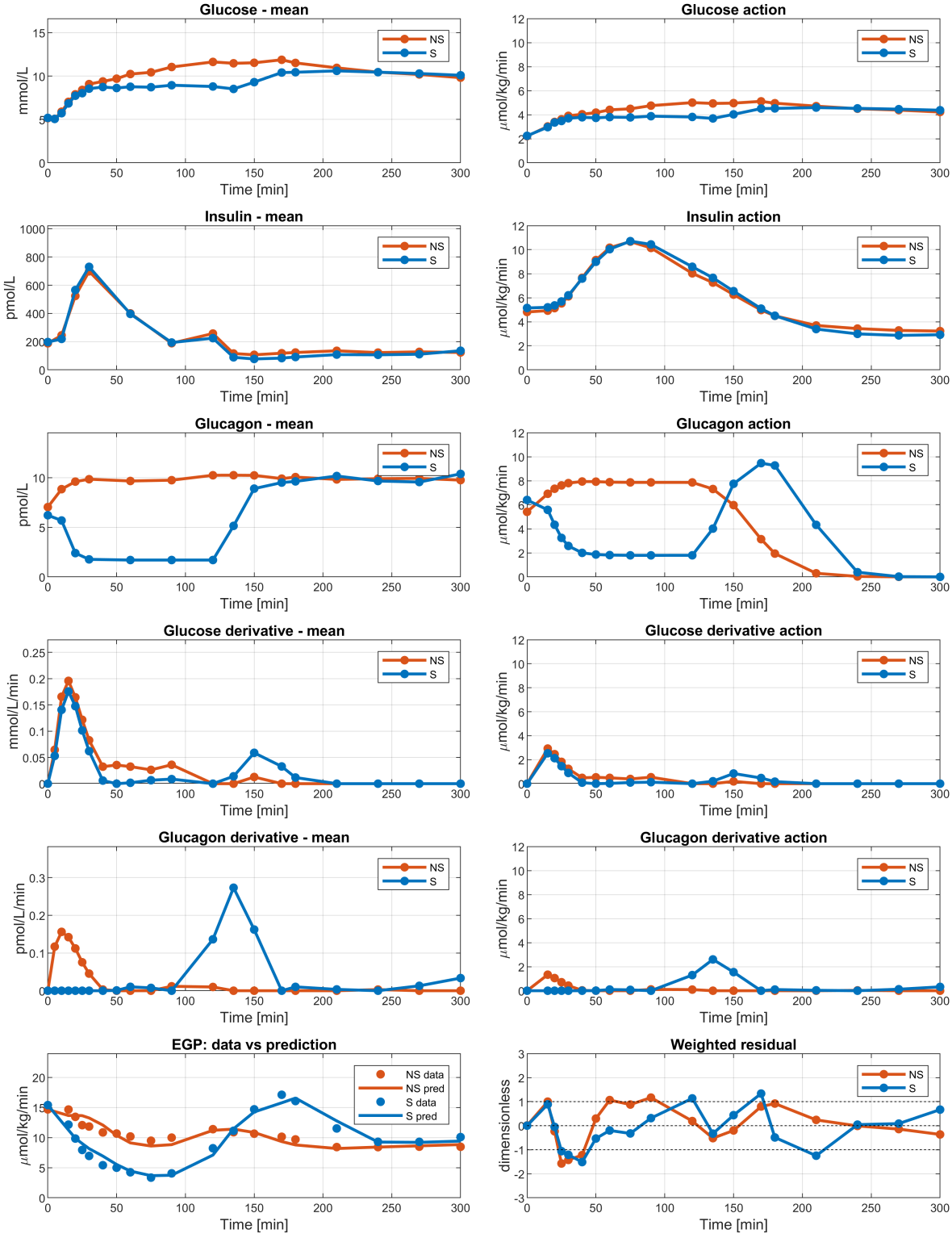

Figure 5.8: Model 8 prediction vs average EGP data: Rows 1-4: input signals (left panel) and relative actions on EGP (right panel); row 5: EGP data vs. model predictions (left panel) and weighted residuals (right panel) in both not suppressed (NS) and suppressed (S) occasions.

	NS		S	
Parameters	**value**	**CV(%)**	**value**	**CV(%)**
kp2 $\left[\frac{ml}{kg \cdot min}\right]$	0.431	31.7	0.434	26.6
kp3 $\left[\frac{\frac{\mu mol}{kg \cdot min}}{\frac{pmol}{l}}\right]$	0.025	20.5	0.026	13.1
kp4 $\left[\frac{\frac{\mu mol}{kg \cdot min}}{\frac{pmol}{l}}\right]$	0.813	16.9	1.054	10.7
kp5 $\left[\frac{1}{min}\right]$	0.039	18.3	0.034	12.8
kp6 $\left[\frac{1}{min}\right]$	0.157	8.4	0.156	0.0
$1/\tau$ $\left[\frac{1}{min}\right]$	0.035	50.1	0.048	43.2
t_0 $[min]$	163.374	8.5	86.145	5.9
kp7 $\left[\frac{ml}{kg}\right]$	14.953	30.6	14.418	24.8
kp8 $\left[\frac{\frac{\mu mol}{kg}}{\frac{pmol}{l}}\right]$	9.387	44.3	9.540	39.5

Table 5.8: Results of Model 8 identified on average data: estimated parameters and their precision (CV) in both not suppressed (NS) and suppressed (S) occasions.

5.2.2 Non linear models of EGP

Non linear model 1

Fitting performance of non linear model 1 (eq. 3.9) was not satisfactory, especially in the S occasion (fig. 5.9). Insulin action profile in NS was not plausible. The a posteriori estimated standard deviation of measurement error v was too high to be acceptable (CV of v will be close to 100% for some data points). For this reasons, this model was discarded.

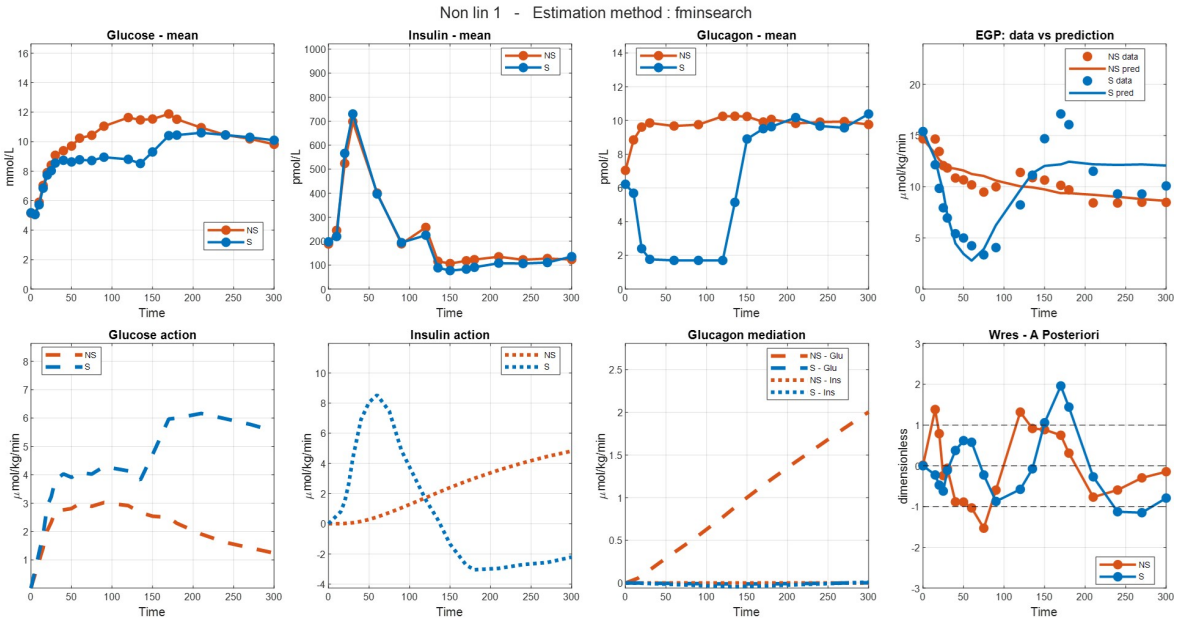

Figure 5.9: Prediction of the non linear model 1 vs average data. First row: input signals and EGP data vs model predictions. Second row: signal actions on EGP and weighted residuals (a posteriori).

Non linear model 2

With respect to non linear model 1, removing the multiplication relationship between glucose and glucagon (as suggested in [12]) did not lead to good fitting results in non linear model 2 (fig. 5.10). This model suffered from the same problems of the previous one, therefore it was rejected.

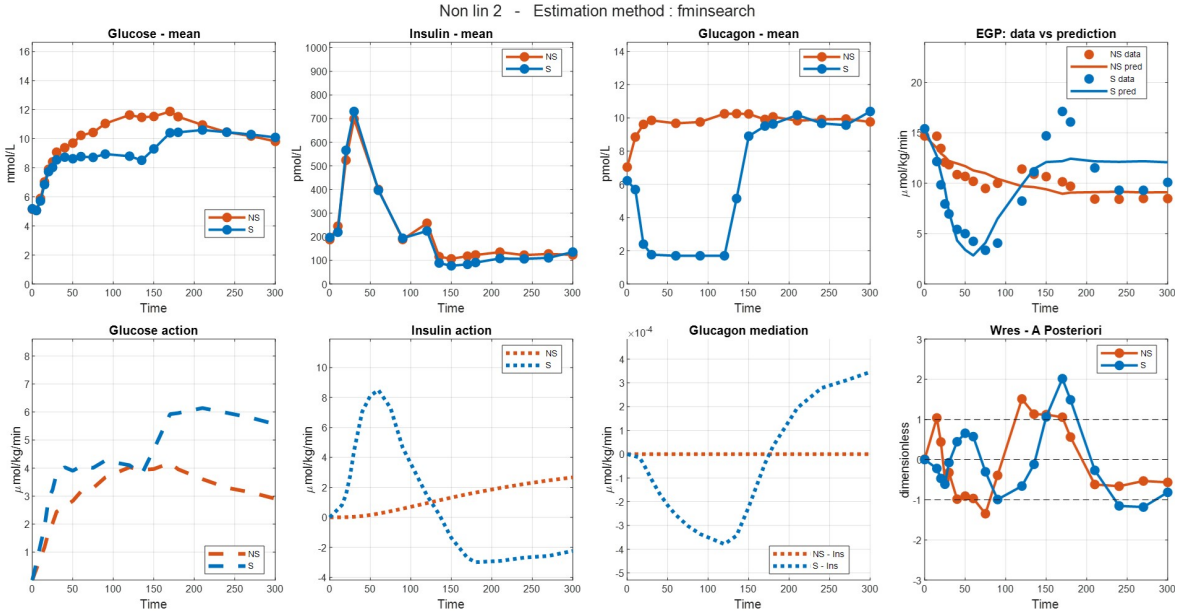

Figure 5.10: Prediction of the non linear model 2 vs average data. First row: input signals and EGP data vs model predictions. Second row: signal actions on EGP and weighted residuals (a posteriori).

Non linear model 3

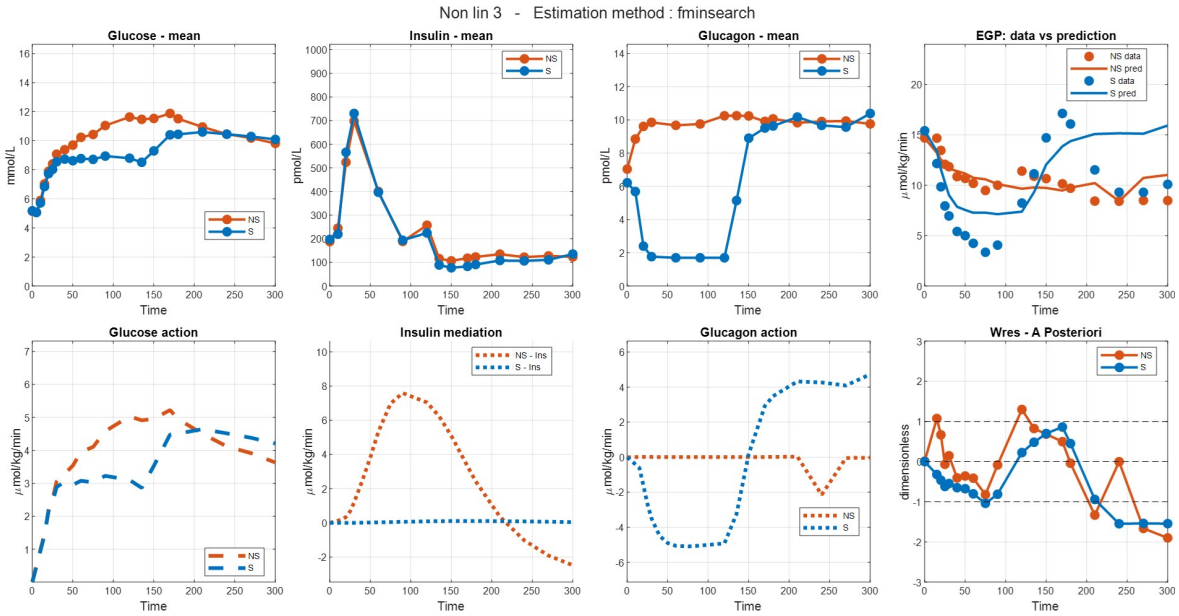

Figure 5.11: Prediction of the non linear model 3 vs average data. First row: input signals and EGP data vs model predictions. Second row: signal actions on EGP and weighted residuals (a posteriori).

Also non linear model 3 produced unsatisfactory results, both in terms of goodness of fit and plausibility of signal actions on EGP (fig. 5.11). Therefore, it was judged not suitable for a proper description of the system.

Non linear model 4

The introduction of glucagon rate of change in non linear model 4 did not produce better results with respect to previous non linear models (fig. 5.12). That's why, also this model was discarded.

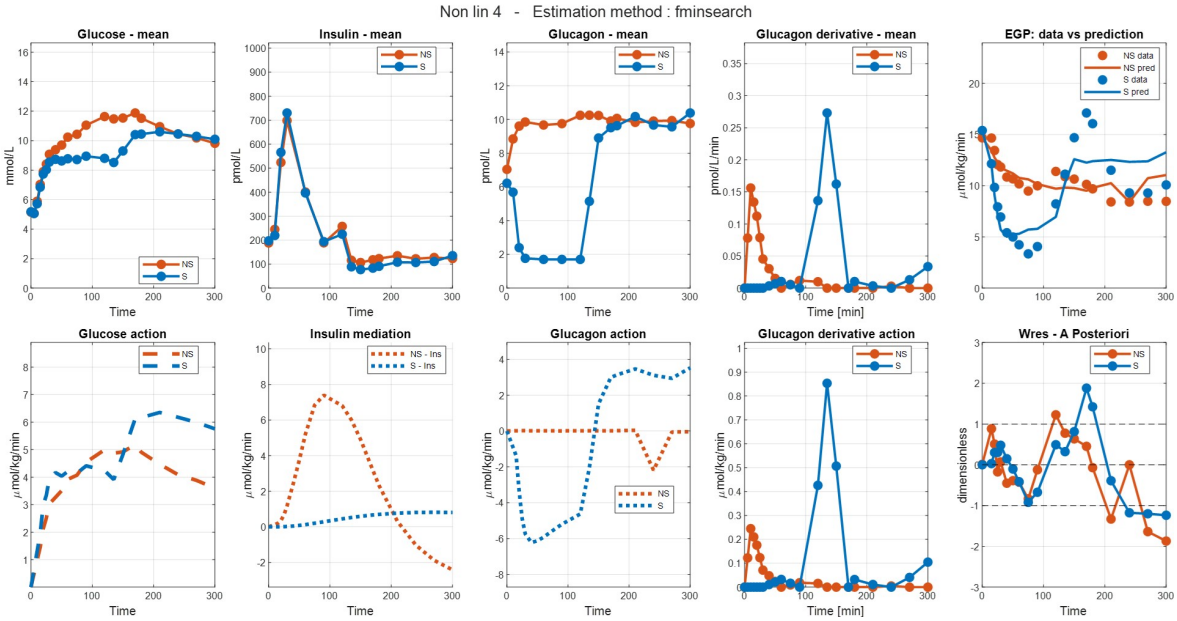

Figure 5.12: Prediction of the non linear model 4 vs average data. First row: input signals and EGP data vs model predictions. Second row: signal actions on EGP and weighted residuals (a posteriori).

5.2.3 Model selection

After model assessment of both linear and non linear models of EGP, it became clear that the best model was to choose among the linear ones. Since there were four models showing good fitting performance and good precision of the estimates (model 4,5,6,8), we compared the metrics like WRSS and parsimony criteria provided by these models.

MODEL	WRSS	GEN-IC	AICc	BIC
4	23.9	38.6	60.4	67.6
5	24.2	38.6	82.1	82.4
6	18.2	34.6	64.4	69.1
8	24.3	49.1	96.3	89.8

Table 5.9: WRSS and parsimony criteria of the 4 best linear models

The best fit (lowest WRSS) was obtained with model 6, that was also the suggested as the best model by GEN-IC. However, both AICc and BIC proposed to choose model 4 (tab. 5.9). Therefore, we decide to test both models on single subject data.
After having tested the two models on individual subject data, we observed that model 6 provided, on average, a better fit than model 4 (figure 5.13 vs figure 5.14 and lower average WRSS, table 5.10). Moreover, all the parsimony criteria (mean values) suggested that model 6 was the best one (table 5.10). Therefore, also at single individual level, it is important to take into account glucose rate of change to predict EGP and therefore **model 6 was selected as the best model of EGP**.

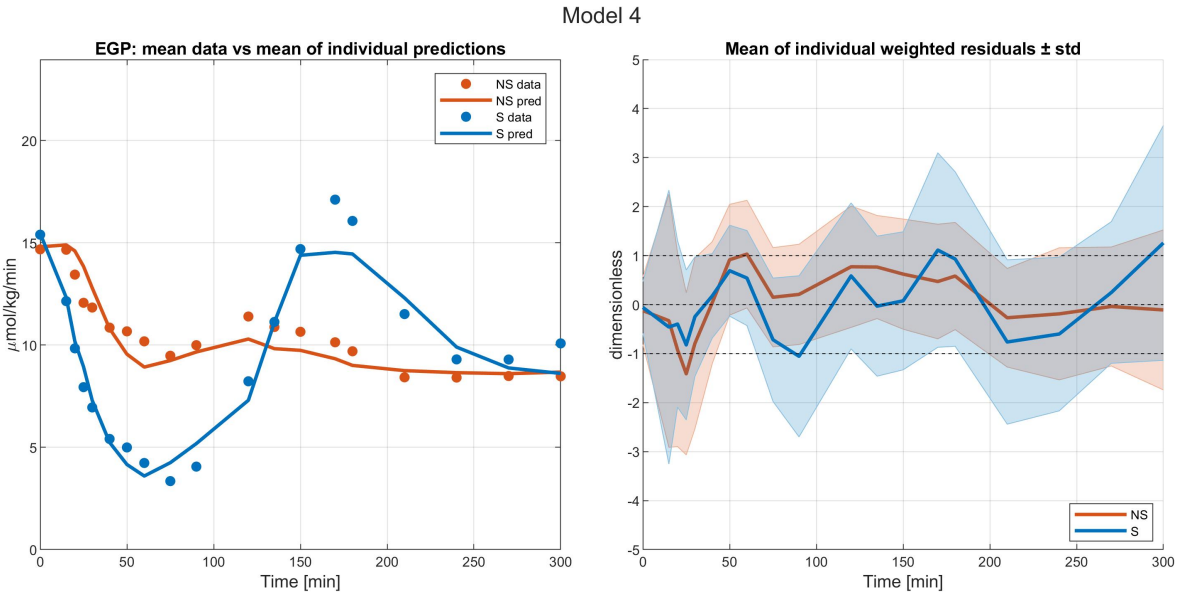

Figure 5.13: Fit of model 4 on single subjects. Left panel: mean EGP data vs average of individual subject predictions. Right panel: mean ± std of individual weighted residuals.

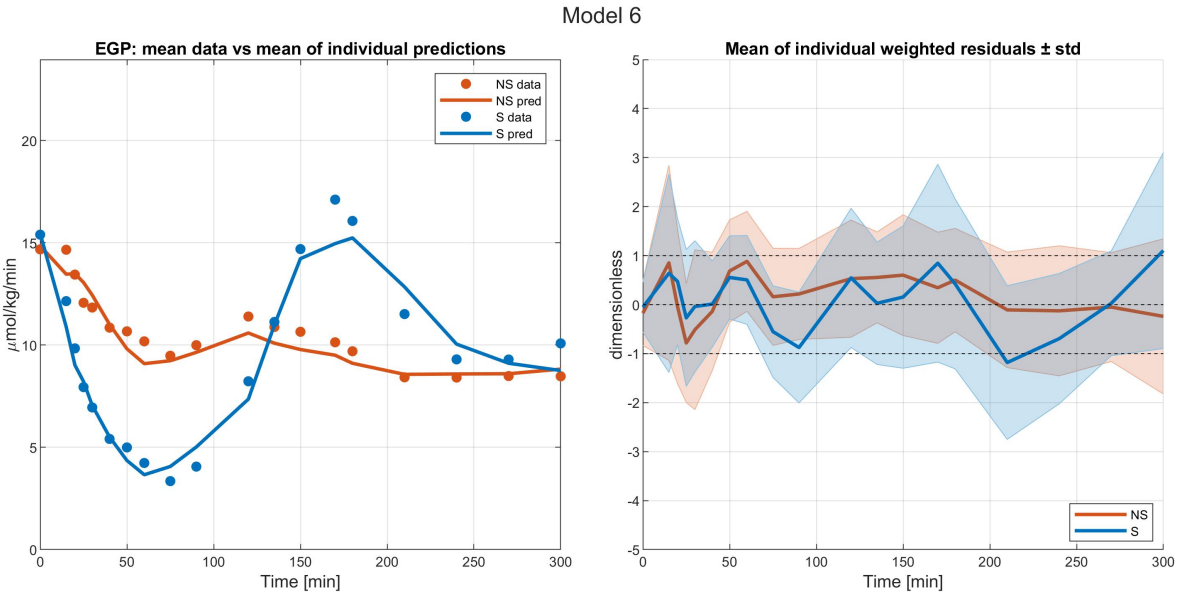

Figure 5.14: Fit of model 6 on single subjects. Left panel: mean EGP data vs average of individual subject predictions. Right panel: mean ± std of individual weighted residuals.

MODEL	WRSS	CV(%)	GEN-IC	AICc	BIC
4	99.1 (±11.5)	27.2 (±7.7)	127.3 (±13.2)	135.8 (±11.5)	142.7 (±11.5)
6	75.6 (±6.4)	37.4 (±18.4)	107.0 (±8.4)	122.2 (±6.4)	126.4 (±6.4)

Table 5.10: Average (±SE) of WRSS, precision of the estimated parameters (CV) and parsimony criteria of model 4 and 6, identified on individual subjects.

5.2.4 Statistical analysis

As highlighted in section 4.1.6, it is interesting to assess if and how much parameters of model 6 changed according to insulin secretion level and glucagon profile. Do to so, a two-way ANOVA was applied.

Levene's test

We have seen that it is important to check if the homoschedasticity hypothesis of ANOVA is satisfied. To do that, we applied a Levene's test. P-values of each parameter grouped by insulin secretion or glucagon infusion (the two factors) is reported in table 5.11. Apart for parameter k_{p7} when is grouped respect to insulin, there is no evidence for rejecting the null hypothesis of the Levene's test (equality of variances of each group). Thus, ANOVA could be used.

	parameters			
factors	**kp2**	**kp3**	**kp4**	**kp7**
Ins. group (0.6/0.8/1.0)	0.069	0.146	0.104	0.0003
Glucagon (S/NS)	0.079	0.094	0.025	0.467

Table 5.11: P-values of Levene's test to check homoschedasticity ($\alpha = 0.05$).

ANOVA

Two-way ANOVA pinpointed that the difference in hepatic glucose sensitivity (parameter k_{p2}) in suppressed (S) vs not suppressed (NS) occasion was statistically significant (p-value = 0.021, table 5.12). The same held for hepatic glucagon sensitivity (parameter k_{p4}) with respect to insulin infusion level (p-value = 0.024). Mean values of k_{p2} and k_{p4} in subjects grouped by insulin and glucagon level are displayed in fig. 5.15 and fig. 5.16, respectively.

	parameters			
factors	**kp2**	**kp3**	**kp4**	**kp7**
Ins. group (0.6/0.8/1.0)	0.684	0.505	0.024	0.102
Glucagon (S/NS)	0.021	0.246	0.117	0.681

Table 5.12: P-values of two-way ANOVA ($\alpha = 0.05$).

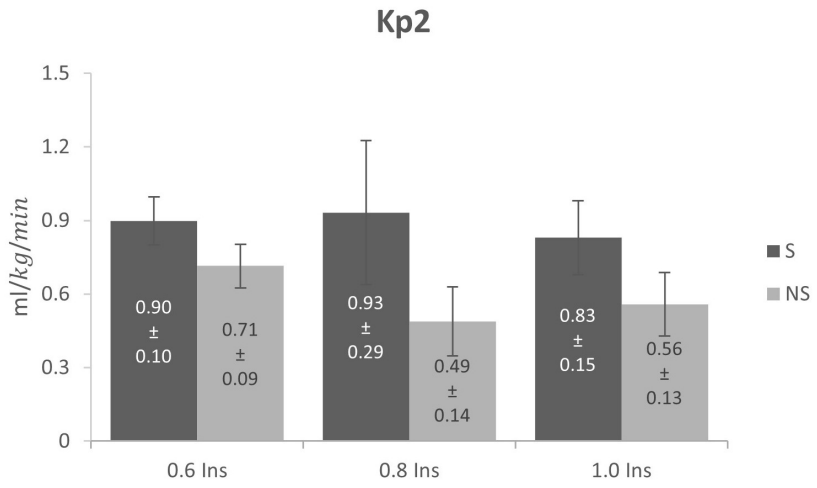

Figure 5.15: Mean hepatic glucose sensitivity (kp2) at low (0.6 Ins), medium (0.8 Ins) and high (1.0 Ins) insulin level in case of suppressed (S) and not suppressed (NS) glucagon. Vertical bars represent standard error.

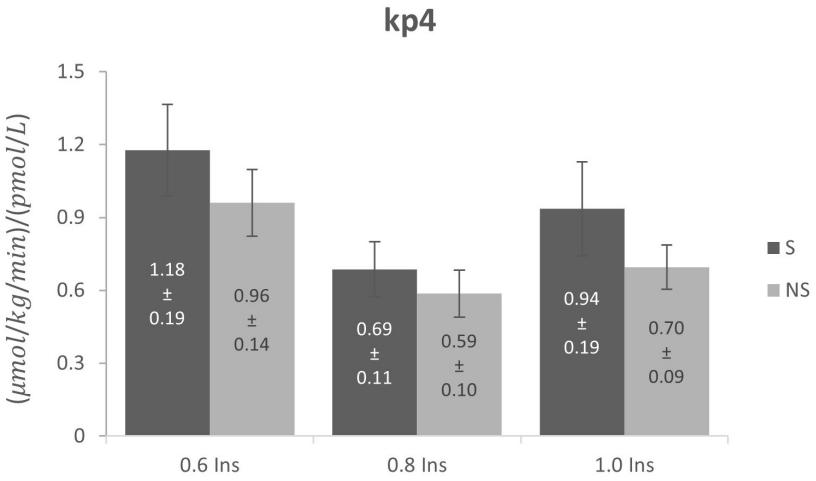

Figure 5.16: Mean hepatic glucagon sensitivity (kp4) at low (0.6 Ins), medium (0.8 Ins) and high (1.0 Ins) insulin level in case of suppressed (S) and not suppressed (NS) glucagon. Vertical bars represent standard error.

Post hoc analysis

ANOVA did not provide details about which group has statistically different values of hepatic glucagon sensitivity (k_{p4}). Consequently, we performed a post hoc analysis to investigate it. We applied a t-test to each insulin group (0.6/0.8/1.0 Ins.) and the results highlight a difference in the group with low insulin level (0.6) with respect to medium insulin level (0.8), as reported in table 5.13. It is worth noting that we did not correct for multiple comparison, since with few data (as in this case), correction may be too strict.

kp4		**Ins group**		
		0.6	**0.8**	**1**
Ins group	**0.6**	-	0.009	0.118
	0.8	0.009	-	0.218
	1	0.118	0.218	-

Table 5.13: P-values of post hoc t-test on parameter kp4 ($\alpha = 0.05$).

Since the t-test showed a robust result (p-value = 0.009), we tried the Tukey's test to correct for FWER. Also with the corrected t-test, group 0.6 and 0.8 Ins resulted having a statistically different glucagon sensitivity of the liver (fig. 5.17). Mean values of group 0.6 and 1.0 were numerically different, however there was too much variability to have a solid difference from a statistical prospective. Probably, increasing the number of subjects in the two groups might produce a more robust difference.

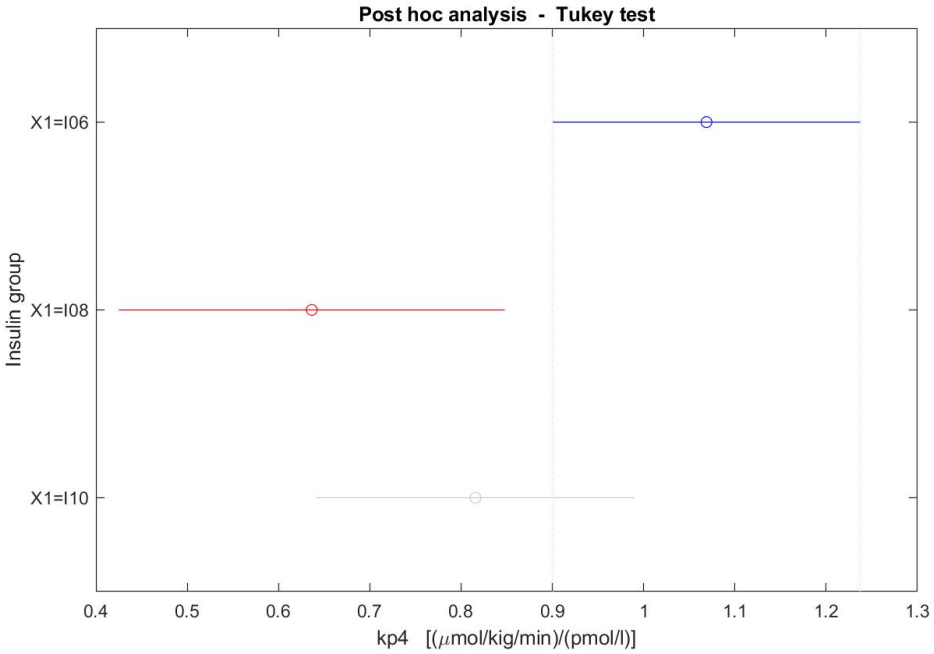

Figure 5.17: Tukey's test on hepatic glucagon sensitivity (kp4). Mean values at low (I06), medium (I08) and high (I10) insulin level. Horizontal bars represent standard error.

Hepatic glucagon action: relationship among parameters

As seen in the physiology section 1.1, a possible explanation for the evanescence effect of glucagon is the depletion of hepatic glycogen. Consequently, an high hepatic glucagon sensitivity (k_{p4}) should lead to a faster reduction of glycogen reserves, which is reflected in a lower value of parameters t_0 and τ (see eq. 3.3 and figure 5.18). As a result, a negative correlation between k_{p4} vs t_0 and k_{p4} vs τ was expected. Scatter plots to evaluate the two relations are depicted in figure 5.19. The expected negative correlation was present in both graphs, in particular the Pearson correlation coefficient (ρ) for k_{p4} vs t_0 was $\rho = -0.26$ (p-value = 0.03), and for k_{p4} vs τ was $\rho = -0.37$ (p-value = 0.002).

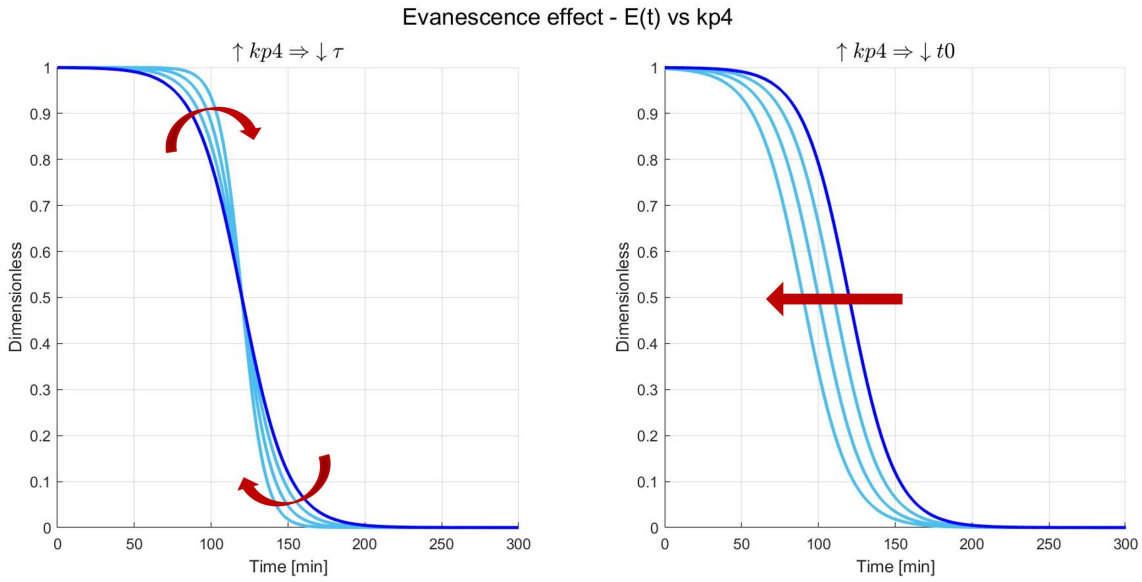

Figure 5.18: Influence of hepatic glucagon sensitivity (k_{p4}) on parameters governing the glucagon evanescence effect (τ and t_0). An higher k_{p4} leads to a faster reduction of glycogen reserves, which is reflected in a lower value of t_0 and τ.

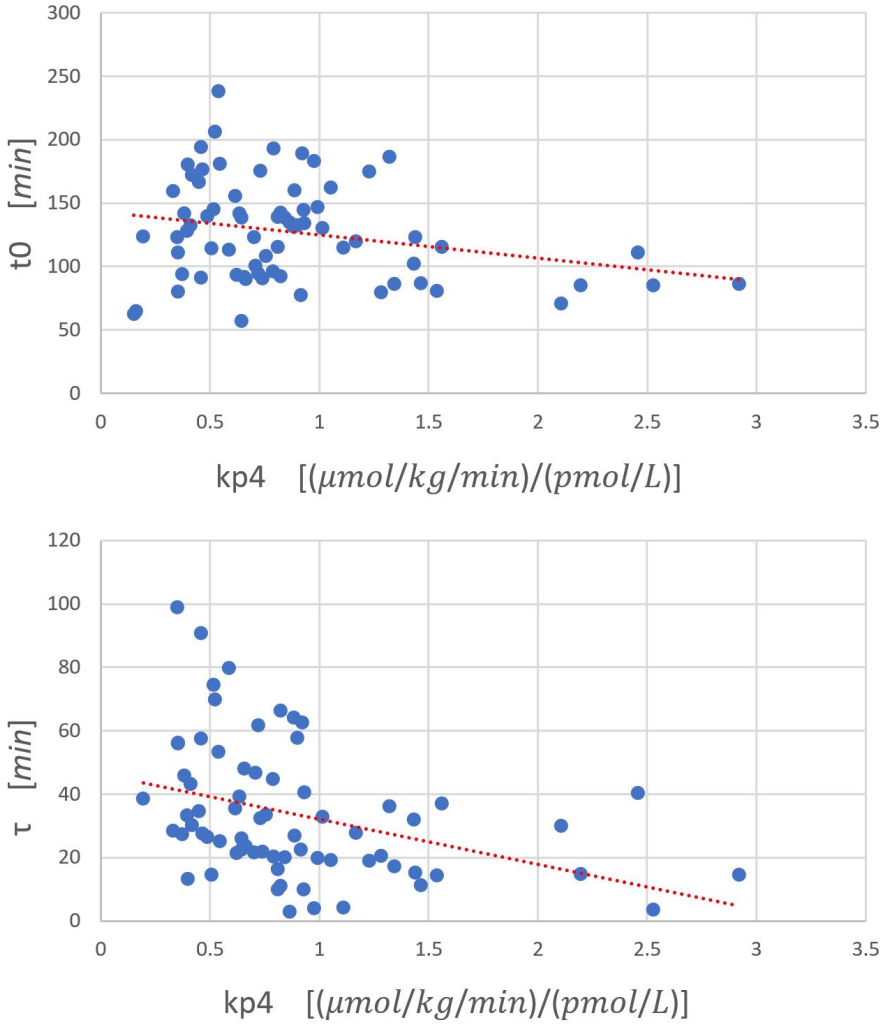

Figure 5.19: Scatter plots of k_{p4} vs t_0 (first panel) and k_{p4} vs τ (second panel).

6

Discussion

As highlighted in the literature review of EGP's mathematical models (section 1.2), simultaneous estimation of insulin and glucagon actions on EGP remains a challenge. A model that addresses this need may be helpful to better describe the pathophysiology of T2DM. In particular, it would be useful to understand how and how much impaired glucagon secretion influences the progression of the disease from a prediabetes condition. In this work, we confirmed that not taking into account glucagon to describe EGP led to poor predictive performance (model 1, section 5.2.1). Moreover, including the glucagon evanescent effect [8] in the model structure was crucial to achieve acceptable fitting performance (model 2 vs model 3, in section 5.2.1). Using glucagon rate of change, as suggested by Emami et al. [26], did not lead to a significant improvement in the prediction of EGP (model 7). Non linear descriptions of the interaction among glucose, insulin and glucagon actions on EGP did not provide satisfactory results (section 5.2.2). The reason may be the increased complexity of the identification procedure due to non linearity (section 4.1.3). In addition, the interpretation of such models is always difficult.
After a careful and systematic comparison of the model performances, we selected model 6 has the best one (section 5.2.3). It assumes that EGP is suppressed by the linear actions of glucose, its rate of change and insulin in a remote compartment, while plasma glucagon stimulated EGP, with an effect that is evanescent. As seen in a previous work [25], also in this study the contribution of glucose rate of change, that is a surrogate of the portal insulin, improved the model. Furthermore, the direct action of plasma glucagon on EGP, and not a delayed version of it ([39],[12]), provided better results. This model formulation is also closer to the physiology. In fact,

the pancreas secretes glucagon into the portal vein, which reaches the liver directly. Thus, it is likely that the glucagon action on the liver is pretty fast.
Statistical results highlighted that in "0.6 Ins" group (corresponding to severely impaired insulin secretion), hepatic glucagon sensitivity S_{Gn} (parameter k_{p4}) was significantly higher than in "0.8 Ins" group (slightly impaired) and than "1.0 Ins" group (p-value = 0.024, fig. 5.16). This demonstrates that glucagon action on EGP is modulated by insulin concentrations, emphasizing the need to quantify secretion and action of both hormones when measuring postprandial pancreatic islets function. In addition, ANOVA highlighted that there was a significant difference in the hepatic glucose sensitivity (also called *glucose effectiveness*, parameter k_{p2} in fig. 5.15) in S vs NS. This result is reasonable, since in the NS occasion glucagon concentration remains high. Thus, from the model prospective, glucose's inhibition action on the liver is less effective with respect to S occasion.
In this study glucose, insulin and glucagon were delivered intravenously into the peripheral circulation. However, the physiological input of the two hormones is the the portal vein. This was an unavoidable limitation, since a direct administration into the portal vein is too invasive and not feasible in humans. It is also important to underline that the evanescence effect of glucagon was modeled with a simplistic approach, according to Hinshaw et al. [12]. For the best of our knowledge, a structural model of this phenomenon (thus, a description more close to the underling physiology) is not present in literature, due to the fact that the mechanism behind this phenomenon is not well understood. A future work should introduce in the model a sophisticated description, when ad hoc experiments that study evanescence will be available. Another improvement may come along with a *population analysis approach*, like non-linear mixed effect models (NLMEM). By converting the selected model into a population one, additional information on the subject can be used, such as anthropometric measurements and genomics data; which are both important factors determining T2DM development ([14],[18]).

A

Introduction to deconvolution

Before taking about deconvolution, it is important to recall some basic concepts about signals and systems. A system, in a broader sense, is a defined object or a part of the space able to modified input signals *u(t)* into output signals *c(t)* in a continuous time setting (the real world). The system is well described by its impulse response $g(t,\tau)$, which is the output of the system when the input is equal to the Dirac delta impulse. When discrete measurements $c(t_k)$ are taken from the output of the system, we moved from continuous to discrete time and usually in the measurement process there is the introduction of some noise v_k. As a result, the final measurement (the collected data y_k) is the sum of the real value and the added noise.

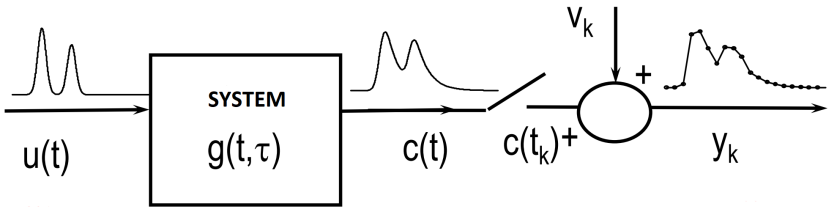

Figure A.1: Discrete measurements $c(t_k)$ of the output $c(t)$ of a general system stimulated by an input signal $u(t)$. Collected data y_k contains also some measurement noise v_k (modified from [43]).

In continuous time, the output of the system is described as the convolution product of the input and the impulse response, that in the scalar case can be written as:

$$y_k = c(t_k) + v_k = \int_{-\infty}^{t_k} g(t_k, \tau)u(\tau)d\tau + v_k \tag{A.1}$$

Where k indicates the k-th measurement.
The aim of a deconvolution process is to travel backwards the chain of causality, so retrieving from the output y_k the input u_k. Making some hypothesis on *u(t)*, such as:

- *u(t)* is a causal signal;
- *u(t)* is constant between two consecutive sampling times.

A matrix-vector model, that describes the input/output relationship of the system, can be realized as:

$$y = c + v = Gu + v \tag{A.2}$$

Where G is the discretized impulse response of the system, also called transfer matrix input/output. y, c, v and u are vectors containing all the data points of the experiment (they have the same dimension). With a least squares estimation, the solution of equation A.2 is:

$$\hat{u}^{LS} = G^{-1}y \tag{A.3}$$

since G is squared and reversible. However, this solution is really sensible to noise since deconvolution is a *ill-conditioned* and also *ill-posed* (not unique solution) problem.

Regularization method

To solve the deconvolution problem, an approach called regularization method was propose by Phillips and Tikhonov in 1962. The idea was to estimate *u(t)* not only with the aim of fitting the data (as in the least squares approach) but also promoting the estimation of a regular signal. Regular means smooth in this case, so a signal that is not oscillating to much (or from the frequency domain prospective, with not to much power in high frequency bands). As a result, the cost function to be minimized to find the estimated input ($\hat{u}^{PT}$) takes into consideration both the adherence of the data and the energy of the m-th derivative of *u(t)*. Since, the more smooth *u(t)* is and the less energy his derivatives have. After some algebraic steps, the solution of this approach is:

$$\hat{u}^{PT} = (G^T B^{-1} G + \gamma F^T F)^{-1} G^T B^{-1} y \tag{A.4}$$

Where B is the covariance matrix of the measurement error (except for a scalar factor σ^2), used to weight each data point with respect to its uncertainty. F is a

matrix that realizes the discrete differentiation of the input signal. Lastly, γ is an hyper parameter that weights the importance of having a smooth estimated signal respect to fitting the data. Consequently, there is the need of a criterion to determine a proper value for γ. In the deterministic setting where we are, a well known criterion is the **Discrepancy Principle**.
The assumptions of this criterion is to knowing σ^2 and to have uncorrelated noise (so B is diagonal). If the assumptions are satisfied, you should selected γ that realizes this equality:

$$r^T r \cong n, \quad r = \frac{y - G\hat{u}}{\sigma B^{0.5}} \tag{A.5}$$

where, $B^{0.5}B^{0.5} = B$. So, the sum of square of the normalized residual (r) should be equal to the number of data (n), or in the same way the sum of square of the weighted residual ($r_w = \frac{y-G\hat{u}}{B^{0.5}}$) should be equal to $n\sigma^2$.
For many reasons, the scalar factor of the covariance matrix of the measurement error can be unknown; in this case you can use other criteria such as:

- Ordinary cross-validation (OCV);
- Generalized cross-validation (GCV);
- L-curve approach.

Also with these approaches some open problems remain. In fact, in a deterministic setting it is not possible to have confidence intervals of the estimated input of the system and to have additional constrains like the non-negative one. To tackle these problems we have to leave the deterministic scenario and move into a probabilistic setting using a **Bayesian approach**.

Deconvolution with a Bayesian approach

with the same model of measurement described in equation A.2, in the new stochastic background u and v are random vectors. A Bayesian approach (more details in section 4.1.2) exploits information on the signals previous to the experiment, the so called *a priori information*. Regarding the error vector v, an usual assumption is an expected value equal to zero and known covariance matrix (a known statistical distribution). Regarding the input vector u, as already mention in the previous section, a regular signal is expected. An usual a priori description is a multi-integrated white noise, for which the covariance matrix can be formalized.

Thus, prior information can be written as:

$$\Sigma_u = \lambda^2 (F^T F)^{-1} \qquad \Sigma_v = \sigma^2 B \tag{A.6}$$

Where λ^2 is the variance of the white noise. The other matrices have the same description of eq. A.4.

A Bayesian approach produces a statistical description about the estimated signal, that is called *a posteriori distribution*. This is even a too rich information since there is not a single estimation provided. Among all possible estimators of u form y, it can be showed that the a posteriori expected value $\hat{u} = E[u|y]$ is the estimator that minimized the sum of square of the estimation error vector of u, ($\tilde{u} = u - \hat{u}$). In case of u and v Gaussian it has an explicit calculation:

$$\hat{u}^{Bayes} = (G^T B^{-1} G + \frac{\sigma^2}{\lambda^2} F^T F)^{-1} G^T B^{-1} y \tag{A.7}$$

It can be appreciated that the formulation of the best estimate of u in a stochastic setting is equal to the estimation of the determinism regularization method (equation A.4), if γ is equal to the ratio of the a priori variances of v and u. As a result, this is the **optimal gamma value** identified with a Bayesian approach:

$$\gamma^{optiman} = \frac{\sigma^2}{\lambda^2} \tag{A.8}$$

Some statistical criteria as been developed to estimate $\gamma^{optiman}$ taking into consideration the amount of known a priori information. If σ^2 is known, γ can be found with the *first consistent criterion*:

$$WESS(\gamma) = \lambda^2 q(\gamma) \tag{A.9}$$

Where *WESS* is the weight estimate sum of squared and q is the trace of a known matrix.

If λ^2 is known, γ can be found with the *second consistent criterion*:

$$WRSS(\gamma) = \sigma^2 n - q(\gamma) \tag{A.10}$$

Where *WRSS* is the weight residual sum of squared.

If both λ^2 and σ^2 are unknown, γ can be found with the *third consistent criterion*:

$$\frac{WRSS(\gamma)}{n - q(\gamma)} = \gamma \frac{WESS(\gamma)}{q(\gamma)} \tag{A.11}$$

References

[1] R. A. DeFronzo et al. *International Textbook of Diabetes Mellitus*. John Wiley & Sons, Mar. 2015.

[2] Jian-Jun Liu et al. "Relationship Between Fasting Plasma Glucagon Level and Renal Function-A Cross-Sectional Study in Individuals With Type 2 Diabetes". In: *Journal of the Endocrine Society* 3.1 (Jan. 2019), pp. 273–283. DOI: 10.1210/js.2018-00321.

[3] Albert L. Lehninger. *Lehninger principles of biochemistry*. W.H. Freeman, 2008.

[4] T. Akhurst. "Chapter 17 - The Role of Nuclear Medicine in the Diagnosis and Management of Hepatobiliary and Pancreatic Diseases". In: *Surgery of the Liver, Biliary Tract and Pancreas (Fourth Edition)*. Ed. by Leslie H. Blumgart et al. Philadelphia: W.B. Saunders, Jan. 2007, pp. 234–265. DOI: 10.1016/B978-1-4160-3256-4.50027-2.

[5] R. A. Rizza, L. J. Mandarino, and J. E. Gerich. "Dose-response characteristics for effects of insulin on production and utilization of glucose in man". In: *American Journal of Physiology-Endocrinology and Metabolism* 240.6 (June 1981), E630–E639. DOI: 10.1152/ajpendo.1981.240.6.E630.

[6] M Bollen, S Keppens, and W Stalmans. "Specific features of glycogen metabolism in the liver." In: *Biochemical Journal* 336.Pt 1 (Nov. 1998), pp. 19–31.

[7] L. Lecavalier et al. "Contributions of gluconeogenesis and glycogenolysis during glucose counterregulation in normal humans". In: *The American Journal of Physiology* 256.6 Pt 1 (June 1989), E844–851. DOI: 10.1152/ajpendo.1989.256.6.E844.

[8] Masafumi Matsuda et al. "Glucagon dose-response curve for hepatic glucose production and glucose disposal in type 2 diabetic patients and normal individuals". In: *Metabolism: Clinical and Experimental* 51.9 (Sept. 2002), pp. 1111–1119. DOI: 10.1053/meta.2002.34700.

[9] Hye-Sook Han et al. "Regulation of glucose metabolism from a liver-centric perspective". In: *Experimental & Molecular Medicine* 48.3 (Mar. 2016), e218–e218. DOI: 10.1038/emm.2015.122.

[10] Dale S. Edgerton and Alan D. Cherrington. "Glucagon's yin and yang effects on hepatic glucose production". In: *Nature Medicine* 19.6 (June 2013), pp. 674–675. DOI: 10.1038/nm.3202.

[11] Steven Russell et al. "Efficacy Determinants of Subcutaneous Microdose Glucagon during Closed-Loop Control". In: *Journal of diabetes science and technology* 4 (Nov. 2010), pp. 1288–304. DOI: 10.1177/193229681000400602.

[12] Ling Hinshaw et al. "Glucagon sensitivity and clearance in type 1 diabetes: insights from in vivo and in silico experiments". In: *American Journal of Physiology-Endocrinology and Metabolism* 309.5 (Sept. 2015), E474–E486. DOI: 10.1152/ajpendo.00236.2015.

[13] *Diabetes Symptoms, Causes, & Treatment | ADA*. URL: https://diabetes.org/diabetes?loc=GlobalNavDB.

[14] Yanling Wu et al. "Risk factors contributing to type 2 diabetes and recent advances in the treatment and prevention". In: *International Journal of Medical Sciences* 11.11 (2014), pp. 1185–1200. DOI: 10.7150/ijms.10001.

[15] William R. Rowley et al. "Diabetes 2030: Insights from Yesterday, Today, and Future Trends". In: *Population Health Management* 20.1 (Feb. 2017). DOI: 10.1089/pop.2015.0181.

[16] P. Shah et al. "Impact of lack of suppression of glucagon on glucose tolerance in humans". In: *The American Journal of Physiology* 277.2 (Aug. 1999), E283–290. DOI: 10.1152/ajpendo.1999.277.2.E283.

[17] P. Shah et al. "Lack of suppression of glucagon contributes to postprandial hyperglycemia in subjects with type 2 diabetes mellitus". In: *The Journal of Clinical Endocrinology and Metabolism* 85.11 (Nov. 2000), pp. 4053–4059. DOI: 10.1210/jcem.85.11.6993.

[18] Meera Shah et al. "TCF7L2 Genotype and α-Cell Function in Humans Without Diabetes". In: *Diabetes* 65.2 (Feb. 2016), pp. 371–380. DOI: 10.2337/db15-1233.

[19] R. A. DeFronzo, J. D. Tobin, and R. Andres. "Glucose clamp technique: a method for quantifying insulin secretion and resistance". In: *The American Journal of Physiology* 237.3 (Sept. 1979), E214–223. DOI: 10.1152/ajpendo.1979.237.3.E214.

[20] C. Cobelli and A. Caumo. "Using what is accessible to measure that which is not: necessity of model of system". In: *Metabolism: Clinical and Experimental* 47.8 (Aug. 1998), pp. 1009–1035. DOI: 10.1016/s0026-0495(98)90360-2.

[21] C. Cobelli and R. Bergman. "Quantitative estimation of insulin sensitivity." In: *American Journal of Physiology-Endocrinology and Metabolism* 236.6 (June 1979), E667. DOI: 10.1152/ajpendo.1979.236.6.E667.

[22] C Dalla Man, A Caumo, and C Cobelli. "The oral glucose minimal model: Estimation of insulin sensitivity from a meal test". In: *IEEE TRANSACTIONS ON BIOMEDICAL ENGINEERING* 49.5 (2002), p. 11.

[23] M. Matsuda and R. A. DeFronzo. "Insulin sensitivity indices obtained from oral glucose tolerance testing: comparison with the euglycemic insulin clamp". In: *Diabetes Care* 22.9 (Sept. 1999), pp. 1462–1470. DOI: 10.2337/diacare.22.9.1462.

[24] Chiara Dalla Man et al. "Measurement of selective effect of insulin on glucose disposal from labeled glucose oral test minimal model". In: *American Journal of Physiology. Endocrinology and Metabolism* 289.5 (Nov. 2005), E909–914. DOI: 10.1152/ajpendo.00299.2004.

[25] Chiara Dalla Man et al. "Use of labeled oral minimal model to measure hepatic insulin sensitivity". In: *Endocrinol Metab* 295 (2008), p. 8.

[26] A. Emami et al. "Modeling Glucagon Action in Patients With Type 1 Diabetes". In: *IEEE Journal of Biomedical and Health Informatics* 21.4 (July 2017), pp. 1163–1171. DOI: 10.1109/JBHI.2016.2593630.

[27] Pau Herrero et al. "A composite model of glucagon-glucose dynamics for in silico testing of bihormonal glucose controllers". In: *Journal of Diabetes Science and Technology* 7.4 (July 2013), pp. 941–951. DOI: 10.1177/193229681300700416.

[28] Sabrina Lyngbye Wendt et al. "Cross-Validation of a Glucose-Insulin-Glucagon Pharmacodynamics Model for Simulation Using Data From Patients With Type 1 Diabetes". In: *Journal of Diabetes Science and Technology* 11.6 (Nov. 2017), pp. 1101–1111. DOI: 10.1177/1932296817693254.

[29] Airani Sathananthan et al. "A concerted decline in insulin secretion and action occurs across the spectrum of fasting and postchallenge glucose concentrations". In: *Clinical Endocrinology* 76.2 (2012), pp. 212–219. DOI: 10.1111/j.1365-2265.2011.04159.x.

[30] A Vella et al. "Effect of glucagon-like peptide 1(7-36) amide on glucose effectiveness and insulin action in people with type 2 diabetes." In: *Diabetes* 49.4 (Apr. 2000), pp. 611–617. DOI: 10.2337/diabetes.49.4.611.

[31] Rita Basu et al. "Use of a novel triple-tracer approach to assess postprandial glucose metabolism". In: *American Journal of Physiology. Endocrinology and Metabolism* 284.1 (Jan. 2003), E55–69. DOI: 10.1152/ajpendo.00190.2001.

[32] Jon D. Adams et al. "Insulin secretion and action and the response of endogenous glucose production to a lack of glucagon suppression in nondiabetic subjects". In: *American Journal of Physiology-Endocrinology and Metabolism* 321.5 (Nov. 2021), E728–E736. DOI: 10.1152/ajpendo.00284.2021.

[33] *Tracer | Encyclopedia.com*. URL: https://www.encyclopedia.com/science-and-technology/chemistry/chemistry-general/tracer.

[34] Aldo Rescigno and Lester Michels. "Compartment modeling from tracer experiments". In: *Bulletin of Mathematical Biology* 35 (Feb. 1973), pp. 245–257. DOI: 10.1016/S0092-8240(73)80024-2.

[35] R. Steele. "Influences of glucose loading and of injected insulin on hepatic glucose output". In: *Annals of the New York Academy of Sciences* 82 (Sept. 1959), pp. 420–430. DOI: 10.1111/j.1749-6632.1959.tb44923.x.

[36] J. Radziuk. "An integral equation approach to measuring turnover in non-steady compartmental and distributed systems". In: *Bulletin of Mathematical Biology* 38.06 (1976), pp. 679–693. DOI: 10.1007/BF02458642.

[37] Elena Breda et al. "Oral Glucose Tolerance Test Minimal Model Indexes of -Cell Function and Insulin Sensitivity". In: *Diabetes* 50 (2001), pp. 150–158. DOI: 10.2337/diabetes.50.1.150.

[38] G. Sparacino and C. Cobelli. "A stochastic deconvolution method to reconstruct insulin secretion rate after a glucose stimulus". In: *IEEE Transactions on Biomedical Engineering* 43.5 (May 1996), pp. 512–529. DOI: 10.1109/10.488799.

[39] Chiara Dalla Man et al. "The UVA/PADOVA Type 1 Diabetes Simulator: New Features". In: *Journal of Diabetes Science and Technology* 8.1 (Jan. 2014), pp. 26–34. DOI: 10.1177/1932296813514502.

[40] C. J. Ramnanan et al. "Physiologic action of glucagon on liver glucose metabolism". In: *Diabetes, Obesity & Metabolism* 13 Suppl 1.Suppl 1 (Oct. 2011), pp. 118–125. DOI: 10.1111/j.1463-1326.2011.01454.x.

[41] Karen B. Schneck et al. "Assessment of glycemic response to an oral glucokinase activator in a proof of concept study: application of a semi-mechanistic, integrated glucose-insulin-glucagon model". In: *Journal of Pharmacokinetics and Pharmacodynamics* 40.1 (Feb. 2013), pp. 67–80. DOI: 10.1007/s10928-012-9287-8.

[42] H. Blauw et al. "Pharmacokinetics and pharmacodynamics of various glucagon dosages at different blood glucose levels". In: *Diabetes, Obesity & Metabolism* 18.1 (Jan. 2016), pp. 34–39. DOI: 10.1111/dom.12571.

[43] Claudio Cobelli and Ewart Carson. *Introduction to Modeling in Physiology and Medicine*. San Diego: Elsevier Science & Technology, 2019.

[44] Giuseppina Bellu et al. "DAISY: a new software tool to test global identifiability of biological and physiological systems". In: *Computer Methods and Programs in Biomedicine* 88 (Oct. 2007), pp. 52–61. DOI: 10.1016/j.cmpb.2007.07.002.

[45] *Fisher information*. URL: https://en.wikipedia.org/w/index.php?title=Fisher_information&oldid=1132788515.

[46] *Anderson–Darling test*. URL: https://en.wikipedia.org/wiki/Anderson-Darling_test.

[47] Sadanori Konishi and Genshiro Kitagawa. "Generalised Information Criteria in Model Selection". In: *Biometrika* 83.4 (1996). Publisher: [Oxford University Press, Biometrika Trust], pp. 875–890.

Acknowledgments

The biggest thanks goes to Prof. Chiara Dalla Man, you were always available for discussion and to answer my questions. I learned a lot from you.
A particular thanks to PhD Marcello Laurenti, with your help I quickly solved many doubts and issues, and to Dr. Adrian Vella for the support in the physiological interpretation in all the stages of this thesis.

Thanks to all of you for the opportunity to draft an abstract about this work, it was a unique experience.

It was a pleasure to work with you.